

BIOCHEMISTRY

Short linear motif candidates in the cell entry system used by SARS-CoV-2 and their potential therapeutic implications

Bálint Mészáros^{1*}, Hugo Sámano-Sánchez¹, Jesús Alvarado-Valverde^{1,2}, Jelena Čalyševa^{1,2}, Elizabeth Martínez-Pérez^{1,3}, Renato Alves¹, Denis C. Shields⁴, Manjeet Kumar^{1*}, Friedrich Rippmann⁵, Lucía B. Chemes^{6*}, Toby J. Gibson^{1*}

The first reported receptor for SARS-CoV-2 on host cells was the angiotensin-converting enzyme 2 (ACE2). However, the viral spike protein also has an RGD motif, suggesting that cell surface integrins may be co-receptors. We examined the sequences of ACE2 and integrins with the Eukaryotic Linear Motif (ELM) resource and identified candidate short linear motifs (SLiMs) in their short, unstructured, cytosolic tails with potential roles in endocytosis, membrane dynamics, autophagy, cytoskeleton, and cell signaling. These SLiM candidates are highly conserved in vertebrates and may interact with the μ 2 subunit of the endocytosis-associated AP2 adaptor complex, as well as with various protein domains (namely, I-BAR, LC3, PDZ, PTB, and SH2) found in human signaling and regulatory proteins. Several motifs overlap in the tail sequences, suggesting that they may act as molecular switches, such as in response to tyrosine phosphorylation status. Candidate LC3-interacting region (LIR) motifs are present in the tails of integrin β 3 and ACE2, suggesting that these proteins could directly recruit autophagy components. Our findings identify several molecular links and testable hypotheses that could uncover mechanisms of SARS-CoV-2 attachment, entry, and replication against which it may be possible to develop host-directed therapies that dampen viral infection and disease progression. Several of these SLiMs have now been validated to mediate the predicted peptide interactions.

INTRODUCTION

The coronavirus disease 19 (COVID-19) pandemic is caused by severe acute respiratory syndrome coronavirus 2 (SARS-CoV-2), an enveloped, single-stranded RNA virus. It had infected more than 68 million people and caused over 1.5 million deaths globally by mid-December 2020. SARS-CoV-2 belongs to the Coronaviridae family, whose members are common human pathogens responsible for the common cold, as well as for some emerging severe respiratory diseases. Among them are the SARS-CoV and the Middle East respiratory syndrome coronavirus (MERS-CoV), the former of which caused over 8000 cases in 2003 with a fatality rate of ~10% and the latter caused about 2500 infections in 2012 with a fatality rate of 37% (1). Another coronavirus, infectious bronchitis virus (IBV), infects birds and has been used as a model in coronavirus research (2). SARS-CoV-2, like SARS-CoV (3), uses the angiotensin-converting enzyme 2 (ACE2) as a receptor (4–6) to attach to host cells. ACE2 is a single-pass type I membrane protein with a short cytosolic C-terminal region for which the functionality, however, is mostly unknown.

Earlier results show that the SARS-CoV-2 receptor-binding domain (RBD) of the spike protein interacts with ACE2 for cellular

entry. In 2004, ACE2 was shown to be highly expressed in lungs by anti-ACE2 antibody staining (7). However, several 2020 papers using both antibodies and single-cell mRNA sequencing now find that there is very little ACE2 gene expression in normal lungs (8–11). This suggests that the ACE2 receptor is insufficient to establish severe lung disease and that SARS-CoV-2 can bind other cell surface receptors on human lung cells. One group of candidate co-receptors are the integrins that bind a large variety of ligands harboring an RGD (Arg-Gly-Asp) sequence motif, as recent analysis of the RBD identified a possibly functional RGD motif (12).

Integrins are major cell attachment receptors, which are known to be targeted by a range of viruses—including HIV, herpes simplex virus-2, Epstein-Barr virus (EBV), and the foot and mouth disease virus (FMDV)—for cell entry and activation of linked intracellular pathways (13–15). Integrins are special types of receptors, as they propagate signals in both directions; extracellular ligands can induce cytoplasmic pathway activation, but intracellular interactions with the cytosolic tails can influence the structure of the ectodomains and hence ligand-binding affinity. The complexity of integrin signaling stems from the dimeric structure of integrins, as they are composed of two subunits, α and β . For the RGD-binding integrins, the ligand-binding surface lies at the interface of the two integrin subunits, with both subunits making contacts with the ligand. These RGD motifs are recognized by at least 8 of the 24 human integrins, and the flanking residues next to the core RGD motif are known to play a decisive role in selectivity (16). Several viral proteins contain RGD (or RGD-like) short linear motifs (SLiMs) for integrin modulation; in addition, not only some viruses can use integrins on the host cell surface but also HIV/SIV (simian immunodeficiency virus) can incorporate integrins into their own membranes for mediating interactions with the host (17). Therefore, integrins can potentially be targeted

Copyright © 2021
The Authors, some
rights reserved;
exclusive licensee
American Association
for the Advancement
of Science. No claim
to original U.S.
Government Works

¹Structural and Computational Biology Unit, European Molecular Biology Laboratory, Heidelberg 69117, Germany. ²Collaboration for joint PhD degree between EMBL and Heidelberg University, Faculty of Biosciences. ³Laboratorio de bioinformática estructural, Fundación Instituto Leloir, C1405BWE Buenos Aires, Argentina. ⁴School of Medicine, University College Dublin, Dublin 4, Ireland. ⁵Computational Chemistry & Biology, Merck KGaA, Frankfurter Str. 250, 64293 Darmstadt, Germany. ⁶Instituto de Investigaciones Biotecnológicas “Dr. Rodolfo A. Ugalde”, IIB-UNSAM, IIBIO-CONICET, Universidad Nacional de San Martín, CP1650 San Martín, Buenos Aires, Argentina.

*Corresponding author. Email: balint.meszáros@embl.de (B.M.); manjeet.kumar@embl.de (M.K.); lchemes@iib.unsam.edu.ar (L.B.C.); toby.gibson@embl.de (T.J.G.)

at both the extracellular and the intracellular side to combat pathogenic hijacking.

Viruses, as obligate intracellular entities, need to interfere with major cellular processes like vesicular trafficking, cell cycle, cellular transport, protein degradation, or signal transduction to satisfy their replication, enzymatic, metabolic, and transport needs (18). To achieve this, a large number of host processes are hijacked using SLiMs often located in intrinsically disordered regions to establish protein-protein interactions with host proteins or undergo post-translational modifications (PTMs) such as tyrosine phosphorylation. For example, cellular signaling relies heavily on the use of SLiMs (19, 20). The low affinity and cooperativity of SLiM-based molecular processes allow reversible and transient interactions that can work as switches between distinct functional states and are regulated in both time and space (21, 22). Conditional switching of SLiMs, for example, through phosphorylation, can induce the exchange of binding partners for a protein, thus mediating molecular decision-making in response to signals reporting on the cell state (20). The Eukaryotic Linear Motif (ELM) resource (<http://elm.eu.org/>) is a dedicated database and exploratory server for over 280 manually curated SLiM classes with experimental evidence, each of them defined by a POSIX regular expression (23).

As explained above, a major strategy of viruses is to abuse the host system by using mimics of eukaryotic SLiMs to compete with extracellular or intracellular binding partners or to sequester host proteins (18). This dependence of viruses and many other pathogens on SLiM-mediated functions suggests that there is an opportunity to drug the cell systems where these interactions are being hijacked (24). For example, tyrosine kinase inhibitors, often used in anticancer therapy, have shown promising coronavirus replication inhibition in infectious cell culture systems (2, 25–27). In the remainder of the introduction, we will describe some of the major pathways hijacked by viruses to accomplish cell attachment, entry, and replication, which are suggested by our results to be relevant to SARS-CoV-2 infection.

Receptor-mediated endocytosis (RME) is a cellular import process triggered by cell surface receptor proteins, including any cargoes attached to them, in which a large vesicular structure is assembled entirely through cooperative low-affinity interactions of SLiMs and phospholipid head groups with their globular protein domain partners. The vesicles are strong and stable, yet flexible and dynamically assembled and disassembled. The external triggering of surface receptors (many of which have the YxxPhi or NPxY tyrosine sorting motifs) is transmitted across the plasma membrane, inducing local enzymatic modification of lipid head groups from phosphatidylinositol-4-phosphate (PI4P) to phosphatidylinositol 4,5-bisphosphate [PI(4, 5)P₂] by the PIPK1 kinase. The local enrichment of PI(4,5)P₂ enables binding of domains such as ENTH in epsins that can begin to curve the membrane and assemble clathrin cages using their clathrin box motif and also attract additional adapter proteins via yet more SLiMs. In turn, additional sets of SLiM-bearing proteins stimulate the actin filament formation and attachment, necessary to fold and pull the invagination into the cytosol. Later, dynamin binds directly to PI(4,5)P₂ on the membrane to complete the scission process. Once in the cytosol, the clathrin-coated vesicles are soon dismantled and the contents are included into the early endosomes. [For recent reviews of the process, see (28–30).] Many viruses enter the cell via endocytosis, using many different cell surface receptors (31). Viruses such as HIV and hepatitis C virus depend on the recognition of more than

one receptor for entry, but in many cases, the stoichiometry of receptor engagement is unknown. Coronaviruses can enter cells through different routes that include RME and cell-cell fusion (32). In the case of SARS-CoV, the main entry route is endocytic and depends on endosome acidification (33, 34). However, protease-mediated activation of the spike protein relieves the pH dependence of viral entry, indicating that acidification is not a requirement per se, but acts by inducing the endosomal cleavage of the spike protein required for viral fusion (35, 36). The spike protein is cleaved either by the transmembrane protease serine 2 (TMPRSS2) at the cell surface or by cathepsin L within endosomes (37). The same entry route and proteases are used by SARS-CoV-2, and the use of endocytosis inhibitors indicates that the main entry route also seems to be endocytic (4, 38).

Autophagy is an evolutionarily conserved process in eukaryotes with multiple cellular roles that include the regulation of cellular homeostasis through the catabolism of cell components, immune development, and the host cell response to infection through pathogen phagocytosis (39). Viruses have evolved mechanisms to block the host cell antiviral response and can further hijack autophagy components to promote their survival and replication. This can be done through viral mimicry of host proteins coordinating autophagy or through the direct inhibition of the host autophagy machinery (40). Coronaviruses exploit the autophagy machinery through different mechanisms (41, 42). For example, MERS-CoV targets the BECN1 autophagy regulator for degradation, blocking the fusion of autophagosomes and lysosomes and protecting the virus from degradation (43). Coronaviruses repurpose cellular membranes to create double-membrane vesicles (DMVs) onto which the replication-transcription complex (RTC) is assembled, a process that involves recruitment of multiple autophagy components (41, 44, 45). DMVs in SARS-CoV-2 confine viral double-stranded RNA (dsRNA) concealing the viral genome from the innate immune system (46). Betacoronavirus mouse hepatitis virus (MHV) RTCs assemble by recruiting LC3-I, a nonlipidated form of the autophagy-associated protein LC3 (microtubule-associated protein 1A/1B-light chain 3) (41, 47), and SARS-CoV RTCs also colocalize with LC3 (44). Proximity-based mass spectrometry on the MHV replication complex further revealed that the RTC environment repurposes components from the host autophagy, vesicular trafficking, and translation machineries (45).

In the present work, we identify a set of conserved SLiM candidates in the ACE2 and integrin proteins, which are likely to act in the cell entry system of SARS-CoV-2 and provide molecular links to understand how the virus recognizes target membranes, enters into cells, and repurposes intracellular membrane components to drive its replication. These molecular links might provide previously unidentified clues toward drugging SARS-CoV-2 infections. We first focus on the extracellular SLiMs, before moving across the membrane to examine the cytosolic potential of the receptor tails. In a coincidentally published paper, experimental testing of several motifs in the receptor tails is presented (48).

RESULTS

Extracellular receptor interplay and viral hijacking in the ACE2/integrin system

The identified RGD motif in the spike protein marks integrins as candidates for acting as co-receptors for SARS-CoV-2 entry. However,

similarly to most SLiMs, the integrin-binding RGD motif has a low sequence information content, and the chance of random occurrence in protein sequences is relatively high. Therefore, the mere presence of an RGD motif in a sequence is not a strong indication of actual integrin binding. However, there are several features that make the spike-integrin interaction via the RGD motif plausible, including sequence- and structure-level information, gene expression profiles, the presence of accessory motifs, and protein-protein interactions. In the next sections, we review how this information gives credibility to the functional nature of the spike protein RGD as an integrin-binding motif and, more generally, to the existence of integrin hijacking by SARS-CoV-2.

The evolution of integrin-binding motif candidates within RBDs in the spike protein highlights that while the RGD motif is not conserved, the integrin-binding capacity might have evolved convergently in several betacoronaviruses. Owing to the high rate of recombination in coronaviruses (49), it is challenging to build proper phylogenies to trace their evolution. However, simply aligning homologs of the RBD from the *Betacoronavirus* genus (Fig. 1A) already shows that the RGD motif candidate is located in a locally less conserved region, hinting at the rapid evolvability of the site. The closest known homolog of SARS-CoV-2 is the RatG13 bat coronavirus containing TGD instead of RGD, which is incompatible with integrin binding. However, while the RGD motif itself is not conserved, several other members of the *Betacoronavirus* genus harbor other possible integrin-binding motifs. SARS-CoV and several of its close homologs, such as BM48-31/BGR/2008, contain KGD at this

site. KGD can bind integrin as part of disintegrin binding, such as in the snake venom barbourin (50), but because disintegrins lacking KGD also bind integrin (51), and there is no evidence of KGD binding independent of disintegrins, we think that SARS-CoV KGD is less likely to be an active integrin ligand.

Considering more distant homologs of SARS-CoV-2, it becomes evident that the presence of an RGD/KGD site is not a universal feature of betacoronaviruses. The RBD of a moderately related *Rousettus* bat coronavirus does not contain any of the three residues of the RGD (Fig. 1B). However, other even more distant coronavirus sequences show a different potential integrin targeting motif at the same site. OC43 is a betacoronavirus that is one of the pathogens causing the common cold. Several OC43 RBD sequences show an NGR motif in nearly the same position as the SARS-CoV-2 RGD. NGR is an integrin interaction motif that becomes active upon the nonenzymatic natural deamidation of the asparagine residue preceding a glycine to isoaspartic acid, forming an L-isoDGR site, which can recognize several α v integrins, as well as integrin α 5 β 1 (52). The parallel evolutionary emergence of potential integrin-binding motifs at this location indicates that, despite the lack of conservation at the site, the SARS-CoV-2 RGD motif might be functional.

Normally, the functional importance of a protein region correlates with its conservation. Checking for sequence variances in the SARS-CoV-2 spike protein RGD motif across isolates showed that all 8841 (when checked on 9 June 2020) high-quality full spike protein sequences in GISAID (Global Initiative on Sharing Avian

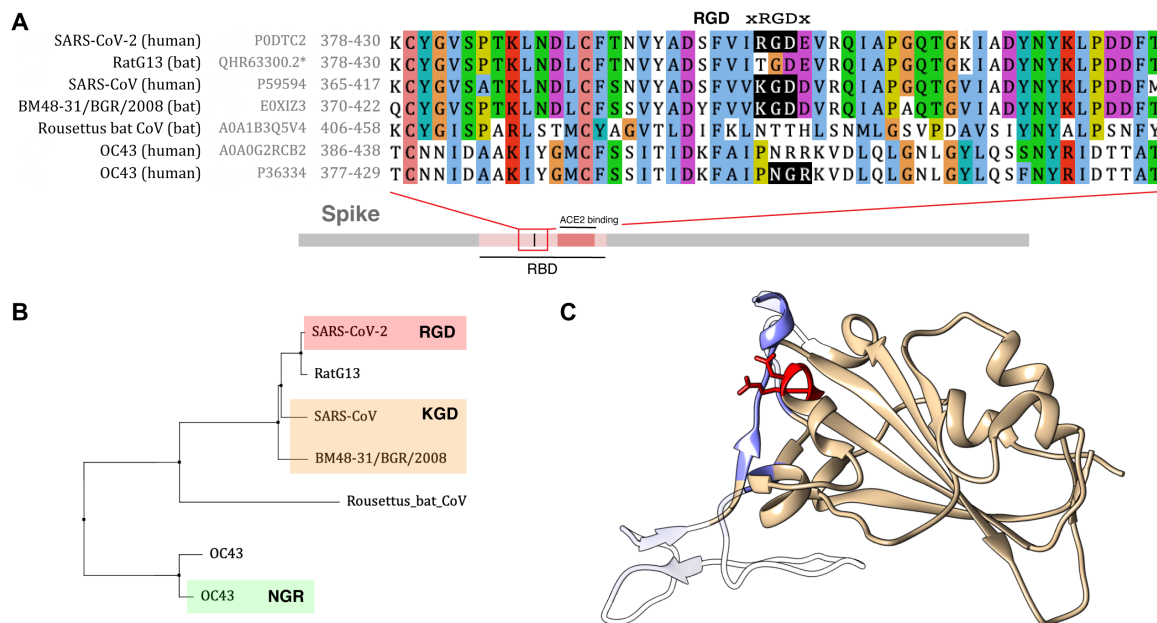


Fig. 1. The RGD motif of the SARS-CoV-2 spike protein. (A) Multiple sequence alignment of a part of the SARS-CoV-2 spike RBD region using homologous sequences from betacoronaviruses of various evolutionary distances and showing the location of potential integrin-binding motifs in black. Virus names together with the host organisms, UniProt accessions (*or GenBank accession in the case of RatG13), and sequence region numberings are shown on the left side of the alignment. The location of the region shown in the alignment is indicated in a representative diagram of the spike protein, together with the location of the RGD motif and the region responsible for ACE2 binding. **(B)** Neighbor-joining tree of the multiple sequence alignment, with this particular set of sequences containing the potential high affinity, low affinity, and reverse integrin-binding motifs (RGD, KGD, and NGR) shown in red, orange, and green boxes, respectively. Only the sequence regions shown in (A) were used in the calculation of the tree. **(C)** Structure of the SARS-CoV-2 RBD as seen in the ACE2-bound form (PDB:6m17). The RGD motif is shown in red sticks. Regions in direct contact with ACE2 are shown in blue. Residues with missing atomic coordinates (indicating flexibility) in the unbound trimeric spike protein structures (PDB:6vbs, 6vxx, and 6vyb) are shown in transparency. Alignment and tree were prepared in Jalview (226) with Clustal colors. Structure was visualized using UCSF Chimera (228).

Influenza Database) (53, 54) contain the RGD region together with the two flanking residues. While normally a fully conserved site would indicate functional importance, the full spike protein sequence shows very little variation among isolates, with some standard conservation scores (55) giving a value of 1 uniformly across the whole spike protein sequence.

The structural features of the SARS-CoV-2 spike protein RGD motif are compatible with integrin binding. At the time of reporting the RGD motif, no SARS-CoV-2 spike protein structures were available, so the authors used structural homology modeling to determine that the RGD motif is surface accessible (12). Since then, several RBD structures have been determined, in both unbound (5, 56) and ACE2 complexed forms using electron microscopy (57) and X-ray diffraction (58), allowing for the direct structural assessment of the possibility of binding to integrins. In the sequence, the RGD motif and the ACE2 binding site do not overlap (see the schematic in Fig. 1A); however, in the RBD structural fold, the RGD motif is largely surrounded by residues binding to ACE2 (Fig. 1C). This indicates that ACE2 binding obscures the RGD motif and the two interactions would be mutually exclusive on a single copy of the RBD. However, in the uncomplexed structures, the residues that surround the RGD site are flexible, whereas the RGD motif is surface accessible and is in the appropriate β -turn conformation for binding integrins. Thus, without ACE2, the interaction with integrins is not sterically blocked.

The spike protein is heavily glycosylated in its functional form. A comprehensive glycosylation analysis of the spike protein showed that the ACE2 binding site can be partially shielded by structurally nearby glycans located at Asn¹⁶⁵, Asn²³⁴, and Asn³⁴³. However, the spike protein RBD has two alternative conformations, and this shielding by glycans only happens in the “down” conformation. Similarly, the glycans do not shield the RGD motif in the binding-competent “up” conformation (5, 59), and therefore, the RGD is accessible for interaction.

Given that the spike protein exists as a trimer on the virion surface, different copies of the RBD can, in theory, interact with ACE2 and integrins at the same time. Under the right structural settings, even two copies of the RBD in the same spike protein trimer can bind to ACE2 and integrins. The feasibility of such an interaction depends on the spatial orientation of the integrin:ACE2 complex, which has been shown to form naturally (60). Although we know that the interaction is between ACE2 and the β subunit of the integrin dimer, there is no solved structure of the ACE2-integrin complex. However, further structural consideration may indicate whether the spike-ACE2 and the spike-integrin interaction can coexist within the same spike protein trimer (fig. S1). The ectodomains of both ACE2 and integrins in the open conformation are roughly the same length measured from the membrane, being about 100 Å, depending on the conformation of the integrin dimer [based on available structures; PDB:6m17 (57) and PDB:6avr (46)]. This means that the RGD-binding site of integrins and the RBD-binding regions of ACE2 are relatively close in space. In addition, in the ACE2 binding-competent up conformation of the RBDs, the distance between pairs of RBDs is about 66 Å [based on the structure PDB:6x2b reported in (61)]. Thus, the simultaneous binding of an integrin dimer and an ACE2 dimer to the same spike protein trimer would orient ACE2 and the integrin to have the correct distance and orientation for the integrin β subunit to bind ACE2.

The sequence and structure context of the RGD motif can indicate possible target integrins. RGD motifs are recognized by several integrins, and specificity is determined mostly by the flanking residues of the core motif. As evidenced by crystallized integrin dimer-ligand complexes, the residue preceding RGD is in contact with the α subunit, whereas the residue after the core motif interacts with the β subunit. The immediate context of the SARS-CoV-2 RGD motif is 402-IRGDE-406 (Fig. 1A), which can give an indication about possible integrin targets. IRGD can be found in several native integrin-binding partners, including FREM1 (62), MFAP4 (63), and IGFBP1/2 (64, 65). These extracellular matrix proteins target integrins with α v, α 5, and α 8 subunits. RGDE is present in the native human integrin ligands TGFBI, ostelectin, collagen α -1(VI) chain, PSBG-9, and polydom, and in vitro and in vivo binding studies of the specificity profiles of these proteins (66–71) highlighted a post-RGD Glu to be efficient in binding to β 1, β 2, and β 3 integrin subunits. Correlating these preferences with possible α - and β -integrin subunit pairings points to the most likely candidate target integrins for SARS-CoV-2 being α v β 1, α v β 3, α 5 β 1, and α 8 β 1. However, in vivo and in vitro integrin-binding studies have indicated that various α v and α 5 β 1 integrins share a large overlap in binding specificity for ligands, and therefore, any of these integrins might play a role in SARS-CoV-2 cell attachment and infection.

Most RGD-binding integrin dimers recognize the partner RGD motif in a long loop conformation that fits into the deep binding pocket of the receptor (fig. S2A), including the integrin candidates identified by the RGD-flanking residues. However, available structures highlight that α v β 6 integrins have a different structural preference in their ligands. In this binding mode, the ligand is only in contact with the integrin α subunit via the Arg residue of the RGD motif. Therefore, the α subunit plays little role in specific ligand recognition. In contrast, the region following the RGD motif adopts an α helix and binds to the β -integrin subunit (fig. S2B). In most known cases, this interaction is stabilized by two small hydrophobic residues fitting into two hydrophobic pockets on the surface of integrin β 6, establishing contacts with the three specificity-determining loops (72), conforming to a pattern of xRGD ϕ xx ϕ , where ϕ indicates a hydrophobic residue and x indicates any residue. This binding mode is known to be used by the growth factors transforming growth factor- β 1 (TGF- β 1) and TGF- β 3 (72), and it is also mimicked by the cell attachment loop of the FMDV for cell entry (73). In its unbound state, the RGD motif of the SARS-CoV-2 spike protein RBD resides in a loop, followed by a helical structure containing two small hydrophobic residues, reminiscent of bound structures of α v β 6 ligands (fig. S2C). While the RBD is stabilized via three disulfide bridges, the RGD motif-containing region is on the far side of the domain. In addition, this region—together with the ACE2 binding site—has the highest average B-factor of the whole spike protein trimer (fig. S2D), hinting at a possible structural rearrangement to accommodate the binding.

A major difference between TGF- β -type ligand and the RBD sequence is that RBD contains an extra residue between the RGD and the two hydrophobics, conforming to a pattern of RGDx ϕ xx ϕ instead. On the basis of current knowledge, it is unclear how this would influence integrin binding; however, there are known α v β 6 ligands that also deviate from the TGF- β subtype. Fibrillin-1 contains an integrin-binding region with the sequence RGDNGD-TACSN, and it is a known ligand for integrins α 5 β 1, α v β 3, and α v β 6 (74). The deviation from the canonical TGF- β -type motif is possibly a compromise between the—hitherto undescribed—specificity

determinants of the three integrins, resulting in binding to several receptors with reduced affinity.

Motif-domain interactions are typically under heavy spatio-temporal regulation. Hence, the SARS-CoV-2 RBD-integrin binding can only occur if the possible target integrins are expressed on the infected host cells. Integrins $\alpha 5\beta 1$ (75) and $\alpha v\beta 3$ (76–78), at least, have been observed in lung epithelial cells—the primary cells of infection in the lung—and are implicated in the emergence and progression of various diseases, including emphysema, non-small cell lung cancer, and mechanical injury of the lungs (79). SARS-CoV-2 infection has been observed to cause damage in various other tissues as well, including the heart, blood vessels, liver, and kidney (80). αv integrins are near ubiquitous in major human tissues (81) and have been observed in all organs with observed damage from SARS-CoV-2 infections.

There are several other factors that point to an interplay between ACE2 and various integrins under normal cellular conditions. It has been shown that in heart tissues, ACE2 is able to bind the $\beta 1$ and $\alpha 5$ subunits of integrins in an RGD-independent manner, enhancing cell adhesion and regulating integrin signaling via the focal adhesion kinase (FAK) (60). It is unclear whether ACE2 interacts with integrins from the same cell, suppressing integrins by locking them in an inactive conformation, or adherent cells, acting as a direct inhibitor of integrins. However, the functional link indicates that integrins and ACE2 are expressed on the surface of the same cells in certain tissues, further corroborated by large-scale expression data (81). Furthermore, the RGD independence of the interaction means that while ACE2 and integrins are in complex, the RGD-binding site of the integrin is unoccupied, leaving it available for a potential interaction with a spike protein trimer.

Apart from the known interplay between ACE2 and integrins, there are additional features that indicate an even tighter cross-talk between the two receptors. RGD-mediated interaction to integrins is metal-mediated (via divalent cations like Mg^{2+} or Mn^{2+}), and all integrins have a so-called “metal ion-dependent adhesion site” (MIDAS) motif (DxSxS) (82). The integrin MIDAS structural motif is located near the ligand-binding site on the β subunit and is essential for binding, as side chains belonging to the motif and an acidic residue from the ligand coordinate the metal ion together (83). ACE2 also has a similar DxSxS motif (see Table 1) that might facilitate interactions with ligands that are recognized by integrins, creating an overlap between the ligand-binding profiles and regulation of the two receptors. In the known structures where spike protein is bound to ACE2, the RGD motif is not in contact with the ACE2 MIDAS (57). However, the MIDAS motif is highly conserved across species (see Fig. 2) and surface exposed. The conserved ACE2 MIDAS motif partially overlaps with a semiconserved NxT glycosylation motif, and the attached carbohydrate is present in solved ACE2 structures (57). This glycosylation does not directly affect the MIDAS’s acidic residue, which might play the main role in ligand binding. Consequently, the ACE2 MIDAS may still be involved in mediating an interaction with an RGD-like motif, potentially serving as a parallel mechanism for binding the spike protein.

Extracellular proteases are native modulators of cell surface receptors, and the SARS-CoV-2 spike protein uses these proteases to enhance infection. ACE2 and several integrin subunits require proteolytic cleavage for biological activity. Integrin subunits $\alpha 3$, $\alpha 5$, $\alpha 6$, and αv are cleaved by furin or furin-like proprotein convertases (PCs) during maturation (84, 85). Nearly all PCs contain an RGD

motif, and while its role in integrin binding is not clear, the motif has been shown to be required for proper functioning for several PCs (86–88). The SARS-CoV-2 spike protein contains a furin-like cleavage site that is absent from closely related spike proteins, immediately following the RBD (89). This cleavage is essential for infection of human lung cells (90) and results in increased virulence. A structural effect of the cleavage might be to allow greater movement of the RBD, potentially aiding in exploring a larger space around the RBD-binding region of ACE2. The cleavage by furin has also been shown to create a new SLiM in the spike protein, conforming to the C-end rule ([RK]xx[R] $\$$ CendR motif where $\$$ indicates the C-terminus of the protein, ELM:LIG_NRP_CendR_1; see Table 1) and mediating attachment to host cell surface via neuropilin-1 and neuropilin-2 (NRP1 and NRP2) (91). Similarly to ACE2, NRP1 physically interacts with integrin $\beta 1$ and regulates integrin signaling (text S1 and fig. S8, A and B) (92, 93). The binding of NRP1 to peptide C termini may be associated with cooperative heparin binding (94); the SARS-CoV-2 S1/S2 cleavage site contains a heparin-binding motif (RRxR) that may partly explain the higher binding affinity of the SARS-CoV-2 spike protein for heparin, compared with SARS-CoV and MERS (95), and the inhibition of SARS-CoV-2 infection by heparin (96).

ACE2 is cleaved by several proteases, including TMPRSS2 (97). ACE2 binds to TMPRSS2, forming a receptor-protease complex (98). TMPRSS2 is also known to cleave the spike protein of both SARS-CoV and MERS-CoV (99), augmenting their entry into the host cell (97). Furthermore, similar results have been found for SARS-CoV-2, where TMPRSS2 was found to be fundamental for cell entry (4). This dependence is most probably twofold: On one hand, TMPRSS2 is needed for ACE2 activation; on the other hand, SARS-CoV-2 spike protein also contains a TMPRSS2 cleavage site (100).

SLiM candidates in the ACE2 receptor intrinsically disordered tail

Recent structural analysis provided experimental evidence that the ACE2 tail is intrinsically disordered across the region following the transmembrane helix (residues 769 to 805) (57), as is also predicted from sequence analysis. The ACE2 sequence (UniProt: ACE2_HUMAN) was entered in the ELM server (23) and returned several relevant candidate SLiMs in the short cytosolic C-terminal tail. Because SLiMs are so short, it is difficult to obtain reliable results in sequence searches. Contextual information, including cell compartment localization and functional relevance, is important in deciding whether a motif candidate is worth testing experimentally (101). Furthermore, in intrinsically unstructured protein sequences, amino acid conservation is usually indicative of functional interactions. Therefore, an alignment was prepared of vertebrate ACE2 proteins. The deepest diverged organism with a sequenced ACE2 gene is the hagfish, a jawless fish included in the subphylum Vertebrata, although it lacks vertebrae (102). All of the detected motif matches in human ACE2 [shown in Table 1 together with potential binding partner domains defined using Pfam (103) and InterPro (104)] were conserved in mammals, most were conserved with birds and mammals and some were conserved with extant reptiles (Fig. 3). These groups diverged from one another >300 million years ago (105). However, whereas the NPY motif, for example, is absent in reptiles, it is present in bony fish ACE2 sequences and also in the hagfish, indicating that NPY has been lost in the reptile lineage. The hagfish sequence shares all of the candidate

motifs present in the human ACE2 tail, although it is >500 million years since their lineages diverged (102). In addition to the strong evolutionary conservation of these candidate motifs, their functional contexts are also biologically coherent, involving signaling by tyrosine kinases, endocytosis, autophagy, and actin filament induction (Table 1). In the following subsections, we briefly summarize each of the conserved motifs and their possible role in the viral entry mechanism.

The ACE2 tail contains a candidate YxxPhi endocytic sorting signal. The YxxPhi motif binds the μ 2 subunit (UniProt: AP2M1_HUMAN) of the endocytosis AP2 adaptors by β -augmentation (106). It is found in numerous cell surface receptors that have intrinsically disordered C-terminal tails (107). A small selection is listed in the database entry ELM:TRG_ENDOCYTIC_2, and while the motif has not been validated in ACE2, it is highly conserved (Fig. 3). When the Tyr is phosphorylated, this motif becomes an SH2-binding site, while in the apo form, it binds the μ 2 adapter. Therefore, this motif can operate as a molecular switch. The residue following the Tyr makes a β -strand interaction and therefore cannot be a proline (PDB:1bxx). The phi position requires a bulky hydrophobic residue. The motif pattern can be represented by the regular expression $Y[\wedge P].[LMVIF]$, and this motif is conserved in ACE2 of all mammals except monotremes. Thus, the mammalian ACE2, which internalizes the coronavirus, has a SLiM candidate for internalization appropriately located within its cytosolic tail. The

ACE2 tail sequence was found to bind with moderate affinity to AP2 μ 2 subunit (48) well within the 30 to 100 μ M range of biologically relevant affinities.

The region encompassing the YxxPhi motif overlaps with a candidate SRC homology 2 (SH2) domain-binding motif (Fig. 3) that is created upon phosphorylation of Tyr⁷⁸¹. SH2-binding motifs are characterized by an invariant phosphotyrosine (pY) that is created following tyrosine kinase activation and allows binding to more than 100 types of SH2 domains present in human proteins (108). The pY residue is accompanied by additional binding determinants that frequently involve hydrophobic residues at the pY + 3 position, but can also involve other combinations, such as Asn at pY + 2 in Grb2-specific SH2 motifs or hydrophobic residues at pY + 4 in STAP-1 SH2 motifs (112; 110). Most SH2 motifs are also characterized by the exclusion of residues at certain positions following the pY, and in general, SH2-binding motifs show a high degree of cross-specificity (112) (109), limiting the power of bioinformatics predictions.

Cell culture infection assays with different coronaviruses, including SARS-CoV, have shown susceptibility to tyrosine kinase inhibitors, indicating the involvement of host tyrosine phosphorylation (25; 26; 27; 2). The sequence found in ACE2 (781-YASID-785) matched the regular expression $(Y)[DESTNA][\wedge GWFY][VPAI][DENQSTAGYFP]$ defined in the ELM database for the SH2 domain present in NCK1/2 proteins, which belong to the class IA SH2 domains (110). No other SH2 entry catalogued in ELM matched the

Table 1. Known and predicted SLiMs in SARS-CoV-2 host-entry interactions. Previously identified motifs are marked with (✓). Regular expressions follow POSIX definitions (23). The symbols 'x' and '.' mark any residues in the definition of main residues and regular expressions.

Region	Protein (UniProt accession)	Motif	ELM class*	Main residues	Regular expression	Start	End	Sequence [†]	Binding domain [‡]	Interaction partner [§]	Interaction type
Extracellular	SARS-CoV-2 spike protein (PODTC2)	RGD	LIG_RGD	RGD	RGD	403	405	RGD	PF00362 and PF01839	RGD-binding integrins, most probably α 5 β 1 and α v β 3	Host:virus
		Multibasic cleavage sites (✓)	–	RRxR	–	682	687	RRAR SV	PF00082 or IPR001254	Furin-like PCs/TMPRSS2	Host:virus
		CendR (✓)	LIG_NRP_CendR_1	RxxR	[RK].[0,2][R]\$	682	685	RRAR	PF00754	Neuropilin-1	Host:virus
	Integrin α v (similar for other α chains) (P06756)	Multibasic cleavage sites (✓)	–	xKR	–	888	892	TKR DL	PF00082	Furin-like PCs	Host
	Integrin β 3 (similar for other β chains) (P05106)	MIDAS (✓)	–	DxSxS	D.[T(S)].S	145	149	DLSYS	–	The acidic part of RGD-like ligands	Host
	Furin (P09958)	RGD	LIG_RGD	RGD	RGD	498	500	RGD	PF00362 and PF01839	Possibly RGD-binding integrin dimers	Host
		MIDAS	–	DxSxS	D.[T(S)].S	543	547	DISNS	–	Unknown partner with acidic residue via metal ion coordination	Host
		Multibasic cleavage site (✓)	–	R	–	697	716	RTEVEKAIRM SRSRINDAFR	IPR001254	TMPRSS2	Host

continued on the next page

Region	Protein (UniProt accession)	Motif	ELM class*	Main residues	Regular expression	Start	End	Sequence†	Binding domain‡	Interaction partner§	Interaction type
ACE2 (Q9BYF1)	I-BAR binding	LIG_IBAR_NPY_1		NPY	NPY	779	781	NPY	IPR027681	I-BAR domain-containing proteins like IRSp53 or IRTKS	
	Endocytic sorting signal	TRG_ENDOCYTTIC_2		Y P xΦ	Y[^P].[LMVIF]	781	784	YASI	PF00928	Adapter protein complex μ2 subunit	
	SH2 binding	-		YxxΦD	((Y)[DE][^AKRHG][DESTAPILVMFYW][^AKR])((Y)[NQSTAILVMFY][^AKRHG][ILV][^AKR])	781	785	YASID	PF00017	SH2 domain of SFKs	
	LIR autophagy	LIG_LIR_Gen_1		ExxYxxΦxΦ	[EDST].{0,2}[WFY][^AKP][^APG][ILMV].{0,4}[LIVFM]	778	786	ENPYASIDI	PF02991	Related proteins LC3, Atg8, GABARAP. There may be some variation in LIR motif specificity	Host
	apoPTB	LIG_PTB_Apo_2		Nxx[FY]	([^P].NP.[FY])([ILVMFY].N..[FY].)	789	796	GENNPGFQ	PF08416	PTB-containing protein with a preference for NxxF core motifs	
	PBM	LIG_PDZ_Class_1		TxF\$	[ST].[ACVILF]\$	800	805	DVQTSF	PF00595	PDZ-containing proteins with TxF\$ preferences such as NHERF3 and SHANK1	
Intracellular	apoPTB (✓)	LIG_PTB_Apo_2		Nxx[FY]	([^P].NP.[FY])([ILVMFY].N..[FY].)	767	774	TANNPLYK	PF00373 PF00630	Talins (high affinity) Dok1 (low affinity) Filamin-A (binding to both apoPTB motifs simultaneously)	
	Integrin β3 (P05106)					779	786	TFTNITYR	PF00373 PF00630	Kindlin Filamin-A (binding to both apoPTB motifs simultaneously)	Host
	PTB (✓)	LIG_PTB_Phospho_1		Nxx(Y)	([^P].NP.(Y))([ILVMFY].N..(Y))	767	773	TANNPLY	PF08416 PF00640 PF02174	Talins (low affinity) Dok1 (high affinity) Shc (binding to both PTB motifs simultaneously)	
	LIR autophagy	LIG_LIR_Gen_1		ExxYxxΦxΦ	[EDST].{0,2}[WFY][^AKP][^APG][ILMV].{0,4}[LIVFM]	777	783	TSTFTNI	PF02991	Atg8 protein family	Host
	ApoPTB (✓)	LIG_PTB_Apo_2		Nxx[FY]	([^P].NP.[FY])([ILVMFY].N..[FY].)	777	784	TGENPIYK	PF00373, PF10480 PF00630	Talins (high affinity) Dok1 (low affinity) ICAP-1 Filamin-A (binding to both apoPTB motifs simultaneously)	
	Integrin β1 (P05556)					789	796	TVVNPKEY	PF00373 PF00630	Kindlin Filamin-A (binding to both apoPTB motifs simultaneously)	Host
	PTB (✓)	LIG_PTB_Phospho_1		Nxx(Y)	([^P].NP.(Y))([ILVMFY].N..(Y))	777	783	TGENPIY	PF10480 PF00640 PF02174	Talins (low affinity) Dok1 (high affinity) ICAP-1 Shc (binding to both PTB motifs simultaneously)	
						789	795	TVVNPKY	PF00640	Shc (binding to both PTB motifs simultaneously)	

*Motif identifier as in the ELM resource. †"|" denotes cleavage points for protease-recognition motifs. ‡Defined through use of Pfam (103) or InterPro (104), where applicable. §SPC, proprotein convertases. ¶ Not a SLiM but a structural motif.

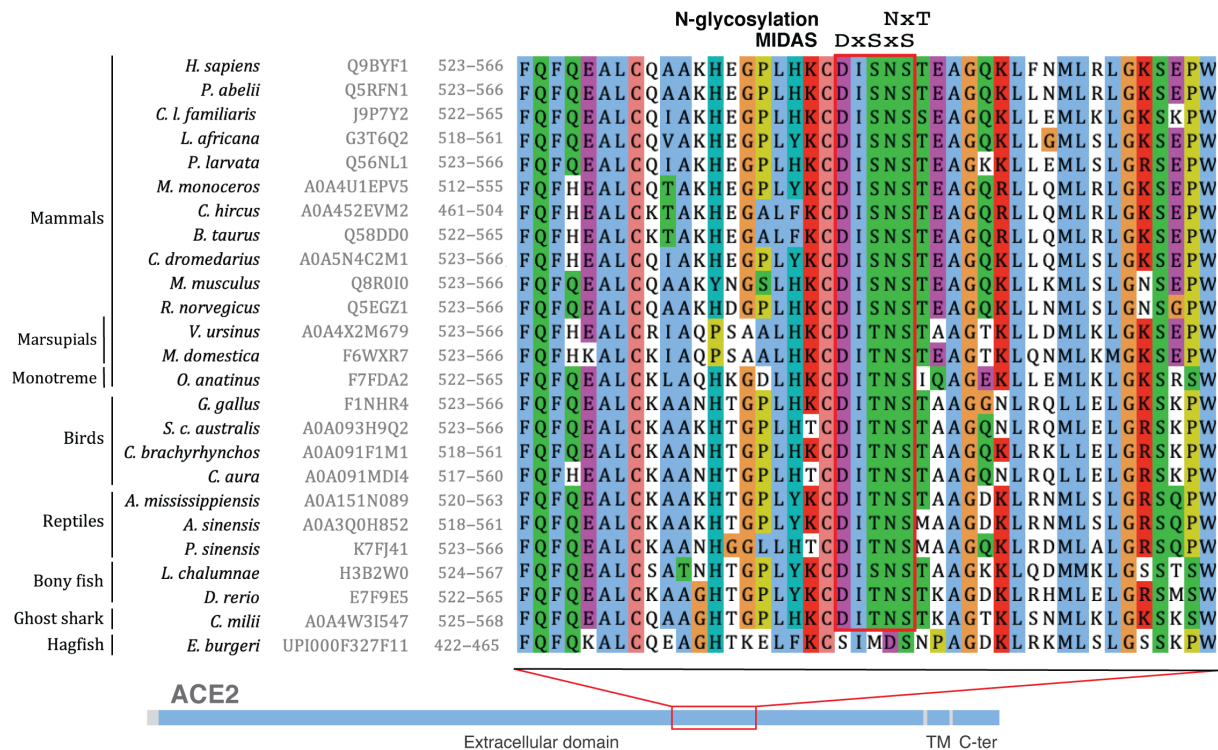


Fig. 2. Alignment of ACE2 illustrating conservation of the MIDAS motif. Multiple sequence alignment of a part of the ACE2 extracellular domain using 25 homologous sequences from different vertebrate lineages (mammals, birds, reptiles, and fish) and showing the conservation of the Dx[ST]xS motif as well as an NxT glycosylation site (main residues displayed above). A red box marks the conservation range of the MIDAS motif in all sequences but the hagfish. Organism names, UniProt IDs (UniParc for hagfish), and sequence numberings are listed on the left side of the alignment. The location of the region shown in the alignment is indicated in a representative diagram of the ACE2 protein. Figure was prepared with Jalview using Clustal colors. TM, transmembrane; C-ter, C-terminal.

tail. Proteins known to contain this motif are listed in entry ELM:LIG_SH2_NCK1_1. We have since learned that an ACE2 phosphorylated Tyr⁷⁸¹ (pTyr⁷⁸¹) tail peptide does not bind to NCK1 (48). Upon re-examination of the SPOT arrays in (111, 112), we noted that the strong preference at pY + 3 is for Val and Pro. While Ile is tolerated at pY + 3 in the context of the high-affinity EPEC Tir (enteropathogenic *Escherichia coli* translocated intimin receptor) sequence (111), it is not tolerated in the context of random peptide pools (112). This would indicate that NCK can only tolerate a weak Ile residue at pY + 3 when a strong residue such as Glu and Asp is found at pY + 1, such as Asp in EPEC Tir. The presence of the weak aliphatic residue Ala at pY + 1 in ACE2 would explain the lack of binding for the ACE2 tail motif. This evidence indicates that the ELM pattern needs correcting to allow only one weak amino acid at either of pY + 1 or pY + 3 in the regular expression.

Other class 1A SH2 domains with a strong preference for Ile at the +3 position in SPOT array include the SH2 domains of the SRC family kinases (SFKs). A regular expression for SRC family SH2 domains allowing for weak/strong residues +1 and +3 positions and compatible with the SPOT arrays could be ((Y)[DE][^KRHG][DESTAPILVMFYW][^KR])((Y)[NQSTAILVMFY][^KRHG][ILV][^KR]) (Table 1). This pattern matches the ACE2 tail. The ACE2 YASID sequence has a weak Ala at pY + 1, neutral Ser at pY + 2, and strong Ile and Asp at pY + 3/+4, making this a plausible motif for binding SFKs. Because all human cells have at least one SFK, and they are involved in regulating endocytosis and actin filament formation (113–115), their SH2 domains are plausible candidates for binding the ACE2 tail. For example, Abl kinases have

specialized cytoskeletal remodeling capacity mediated through their actin binding and actin bundling domains (113), while SRC enhances receptor endocytosis and focal adhesion (FA) remodeling through the phosphorylation of Eps8 and dynamin2 (115). We also turned to the ModPepInt server that uses unsupervised learning techniques to train SH2-binding motif prediction. ModPepInt has models for 51 SH2 domains (116). A run of the ACE2 tail sequence returned best matches with several nonreceptor tyrosine kinases, most harboring class IA SH2 domains that largely overlap with expectations from the SPOT arrays (the kinases Abl1/2, BLK, FGR, FRK, HCK, LCK, SRC, FYN, and TEC) plus other predicted binders, such as the kinase FES and the adaptor proteins GRB10 and GRB14 (table S1). Kliche *et al.* then tested the revised SH2 motif assignment to the SFKs, measuring a low micromolar affinity for the Fyn SH2 domain with the tyrosine-phosphorylated ACE2 peptide (48).

The residues present at pY + 1, pY + 2, and pY + 4 should rule out that the ACE2 YASID motif can be a strong Grb2, CRK, and STAP-1 SH2 domain binder, and binding to SH2 domains in the transcription factors signal transducer and activator of transcription 1 (STAT1), STAT3, and STAT5 is also unlikely due to the lack of adequate specificity determinants. However, other SH2 domains, particularly ones with low observed specificity (e.g., PTPN11_N, PLCgamma1_C, and SH2D1A), could be recruited by ACE2 when there is coexpression in the same cell type. Experimental validation will be required to test these hypotheses.

Tyr⁷⁸¹ in ACE2 also overlaps with a candidate phosphorylation-independent NPY IBAR-binding motif (ELM:LIG_IBAR_NPY_1). This motif was initially described in the bacterial secreted protein

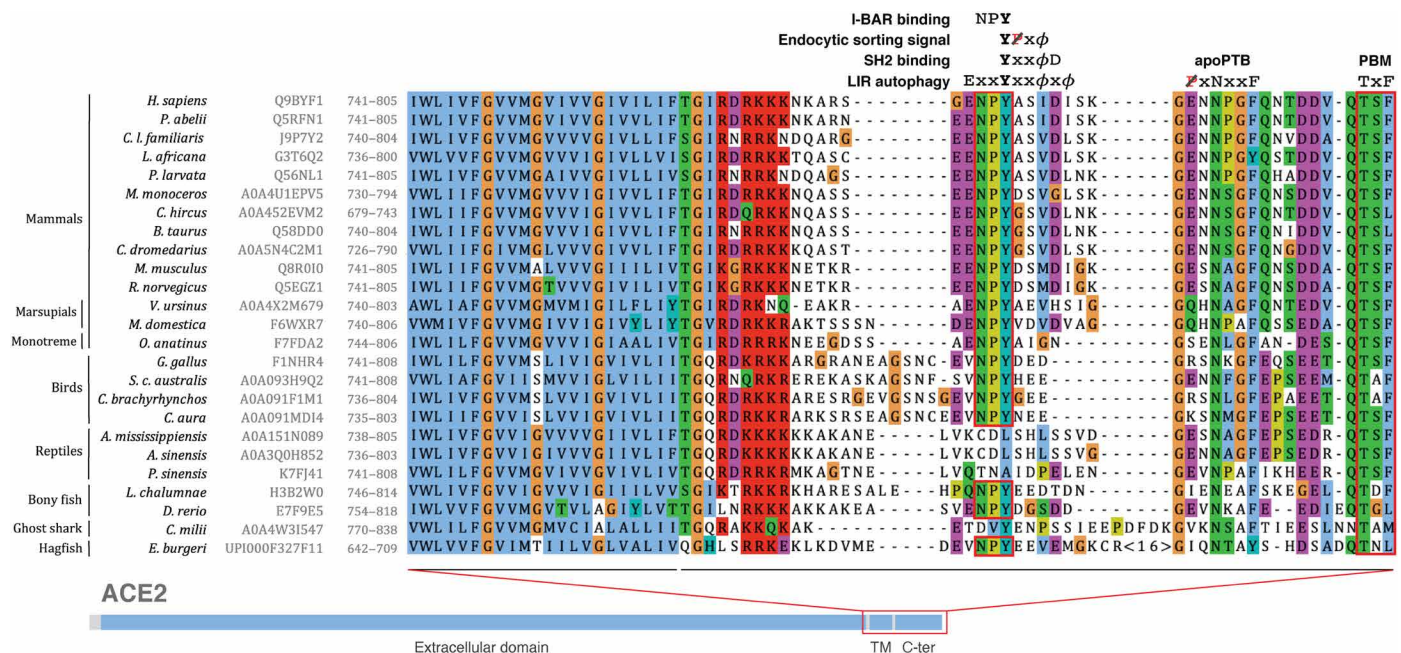


Fig. 3. Alignment of ACE2 illustrating conserved motifs in the cytosolic C-terminal tail following the transmembrane helix. Multiple sequence alignment of ACE2 transmembrane and C-terminal regions using 25 homologous sequences from different vertebrate lineages (mammals, birds, reptiles, and fish) and showing their motif conservation. The names (bold) and key residues of the motifs are displayed above the alignment (ϕ stands for a bulky hydrophobic residue), including a conserved tyrosine (bold) and excluded positions (red and crossed). Red boxes mark the conservation range of the PDZ-binding motif (PBM) (all sequences) and NPY motif (in mammals, birds, and some fish). Organism names, UniProt IDs (UniParc for hagfish), and sequence numberings are listed on the left side of the alignment. The location of the region shown in the alignment is indicated in a representative diagram of the ACE2 protein. Figure was prepared with Jalview using Clustal colors.

Tir from pathogenic strains of *Escherichia coli*, such as enterohaemorrhagic *E. coli* (EHEC). The NPY tripeptide recognizes and binds with a 60 μ M affinity to inverse Bin-Amphiphysin-Rvs (I-BAR) domains in adaptor proteins like insulin receptor substrate protein of 53 kDa (IRSp53) and its homolog insulin receptor tyrosine kinase substrate (IRTKS) (117, 118). I-BAR domains bind to the plasma membrane to favor weak membrane protrusions, and the preference of I-BAR domains for negative membrane curvatures enables a positive feedback loop that can result in the formation of lamellipodia, filopodia, and other types of membrane protrusions (119–121). IRSp53 and IRTKS are modular proteins that contain SH3 domains that, in turn, recognize PxxP SLiMs in actin filament regulators like Mena, Eps8, and mDia1 (122), resulting in the formation of membrane protrusions through actin filament formation (117, 119–121). Moreover, IRSp53 has an additional Cdc42-binding motif that can result in a direct neural Wiskott-Aldrich syndrome protein activation (122). During EHEC infection, the bacteria use the NPY motif in the transmembrane protein Tir to recruit IRSp53 (117). IRSp53 acts as a scaffold to localize the injected bacterial protein EspFU to the bacterial attachment site, cytosolic side, through the binding of a PxxP motif in EspFU to the IRSp53 SH3 domain. Through the use of the same helical SLiM present in NCK (ELM:LIG_GBD_CHELIX_1), EspFU acts as a potent Wiskott-Aldrich syndrome protein activator, inducing the actin polymerization that contributes to the pedestal formation characteristic of EHEC infections (123, 124). The NPY SLiM, although not yet experimentally validated in any human protein, is potentially functional in proteins like SHANK2 or the microtubule-binding CLIP-associating protein 1 (CLASP1), based on protein conservation and functional association (118). The putative NPY motif in ACE2 is conserved in all an-

alyzed mammalian and bird homologs (Fig. 3), suggesting a direct interaction with host I-BAR-containing proteins such as IRSp53 or IRTKS, which are expressed in lung tissues (81).

The I-BAR domain-binding motif in the cytosolic region of ACE2 could be relevant for SARS-CoV-2 infection in the following scenario. During viral cell entry, the NPY motif could recruit I-BAR-containing proteins such as IRSp53 or IRTKS, resulting in membrane protrusion formation that could be exploited for viral entry or in cell to cell transmission. It is known that the hijack of the filopodia formation network is beneficial for the entry and spreading of many enveloped viruses (125), but whether this process is active during coronavirus infection is still unclear. A second route might cooperate with the NPY motif in the recruitment of actin cytoskeleton components. A direct interaction between the SARS-CoV spike protein cytosolic side C-terminal domain and the ezrin FERM (4.1 protein, ezrin, radixin, moesin) domain can occur during the opening of the viral fusion pore and has been proposed to restrain viral infection (126). Ezrin is a protein involved in cell morphology and apical membrane remodeling that acts as a membrane-cytoskeleton linker. Ezrin recruits F-actin through its C-terminal domain and can also bind to IRSp53 located at negatively curved membranes (127, 128), suggesting that while the NPY motif acts at earlier stages of viral attachment, the spike protein-Ezrin interaction might work during or after viral fusion, to promote the recruitment of actin-regulatory components to viral fusion sites.

Apart from the endocytic sorting signal, the SH2 binding, and the IBAR-binding motif, Tyr⁷⁸¹ is also part of an LC3-interacting region (LIR) autophagy motif candidate (Fig. 3). Autophagy, the recycling of cellular material, is vital for cellular homeostasis. Many pathogens must control the autophagy response to establish productive

infection (39). It has been shown that coronaviruses, including those that infect humans, subvert autophagy components to promote viral replication at DMVs associated to the RTC (43, 47, 129, 130). The LIR motif is required for the interaction of a target protein with autophagy-related protein Atg8 in yeast, or its homologs LC3 and GABARAP in human, to facilitate autophagy of the target via the autophagosome (131). The LIR motif has been catalogued in the ELM resource entry ELM:LIG_LIR_Gen_1, and ELM detected a candidate motif in the human ACE2 cytosolic tail sequence (Fig. 3). After the LIR motif was annotated in ELM, a more recently solved LC3-LIR structure (PDB:5cx3) showed that the interacting peptide is longer, with one or two additional hydrophobic interactions (132). LIR enters a hydrophobic groove bordered by positively charged residues. A core [W_FY]xx[ILMV] enters the deepest part of the groove. On either side of the core, the interacting residues can be flexibly spaced. The core must be preceded by a negatively charged residue (which might be enabled by phosphorylation). Furthermore, the motif core is followed by a flexibly spaced hydrophobic residue. There is often a negatively charged residue preceding this hydrophobic position: It can make favorable interactions with counter charges but is not an absolute requirement, so is not included in the revised motif pattern. On the basis of the structure (PDB:5cx3) and some SPOT arrays (132–134), the updated regular expression [EDST].[0,2][W_FY][[^]RKP][[^]PG][ILMV].[0,4][LIVFM] matches the motif instances annotated in ELM. This revised motif is conserved in the mammalian ACE2 cytosolic tail as well as hagfish and ghost shark, but not in birds, reptiles, or bony fish. The ACE2 LIR motif candidate can potentially enable the incoming coronavirus to attract autophagy elements such as LC3 to the structures where the virus replicates and assembles. In line with this, a nonlipidated form of the LC3 protein has been shown to be associated with the RTCs of MHV and SARS-CoV (41, 44, 47). This brings up the interesting possibility that ACE2 remains associated with the membranous structures where SARS-CoV-2 replicates at later infection stages, assisting in the repurposing of autophagy components required for viral replication. Technical issues hampered the comprehensive testing of phosphorylated ACE2 peptide sequences containing the LIR candidate, but the unphosphorylated peptide did not show meaningful binding (48). However, phosphorylation of Ser⁷⁸³ seems to induce a weak binding with MAP1LC3A and GABARAP2 domains, albeit with affinities not reaching physiological relevance (48). So far, the evidence is not enough to support LIR functionality but perhaps multiphosphorylation and/or a longer tail sequence could deliver a stronger interaction.

The ACE2 tail region C-terminal to the overlapping motifs centered around Tyr⁷⁸¹ contains two additional motif candidates. The first such candidate is an apoPTB domain-binding motif. Certain members of the large PTB domain family were initially discovered to bind to phosphorylated NPxY motifs, hence the designation “phospho-tyrosine binding domain” (135). The NPxY motifs in cytosolic tails of receptors, including integrins, are regarded as endocytosis sorting signals (107). It was later discovered that PTB domains in the endocytic internalization adapter protein Dab1 could also bind nonphosphorylated Nxx[FY] motifs (apoPTB motif) and that this might be the case for the majority of PTBs (136). Representative receptors with apoPTB motifs are in the database entry ELM:LIG_PTBApo_2. The core Nxx[FY] motif is conserved in all the vertebrate ACE2s (Fig. 3). For the Dab1 endocytic adapter class

of apoPTB motifs, there is a hydrophobic requirement two residues before the Asn. In ACE2 of fishes such as the hagfish and coelacanth (*Latimeria chalumnae*), the residue is hydrophobic (Fig. 3), suggesting that this motif is present. However, in most other species including human, Glu predominates at this position: Therefore, if this notably conserved Nxx[FY] is an apoPTB motif, it should then bind a PTB protein other than the Dab1 class. The apoPTB motif binds as a short β -strand (β -augmentation) followed by a β -turn. Proline is rejected at the first position of the motif, which is a strand-forming residue, and therefore, the minimal regular expression for this motif is [[^]P].N.[FY]. As with the phosphorylated versions, the apo-motifs are tightly connected to endocytosis (136). The conservation of this motif in the homologous position of the cytoplasmic chain of the partially collinear collectrin protein (UniProt: CLTRN_HUMAN; fig. S3) indicates that this motif instance has an even earlier evolutionary origin than the origin of ACE2 itself, hinting at a key role in internalization. As expected, because the specificity is not yet defined, Dab1 and four other tested PTB domains did not bind to the ACE2 tail region (48). A poorly soluble sorting nexin 17 (SNX17) FERM domain was found to bind with ≈ 100 μ M affinity, providing an ambiguous result.

The very C-terminal region of ACE2 contains a TxF\$ PDZ-binding motif (PBM) candidate. Among other motif-binding modules, PDZ domains come in great abundance in human and other multicellular animals (137). PDZ domains take part in a variety of biological processes including cellular signaling and activity at the neuronal synapse (138). These domains bind by β -strand augmentation to SLiMs that are called PBMs, most commonly known to be found in the C terminus of fully or partially disordered proteins. These interactions are widely studied and their link to various diseases and infections has been previously established (139). A PBM candidate is also found in the very C terminus of the cytosolic tail of all vertebrate ACE2 proteins (Fig. 3). Motifs following a pattern [ST].[ACVILF]\$ are a common PBM variant, described in the ELM resource entry ELM:LIG_PDZ_Class_1. There are multiple functional examples of this motif. However, in the ACE2 protein, the matching sequence has not been characterized. Because the tail of ACE2 is facing the cytosol, it is available to interact with PDZ domains with the appropriate specificity (138).

Two PDZs in two different adapter proteins—Na(+)/H(+) exchange regulatory cofactor NHERF3 and SH3 and multiple ankyrin repeat domains protein 1 SHANK1—have been previously identified to be able to bind TxF\$ sequences (140), which makes both of them candidates for an interaction with the ACE2 C terminus. NHERF3 is colocalized with ACE2 in intestinal tissue, and its PDZ domains were previously validated to interact with PBMs in transmembrane proteins on the cytosolic side of the membrane (141), so it is possible that they come in proximity with the ACE2 tail containing the TxF\$ motif and possibly bind it as a part of ion exchange regulation of small-molecule transport activities. NHERF3 is known for its involvement in sodium ion-dependent transporter activity (142), and ACE2 was also shown to interact with a sodium-dependent transporter (57), which could be one of the leads toward unraveling the possible interaction between NHERF3 and ACE2. Kliche *et al.* (48) confirmed ACE2 tail binding with good affinity for both NHERF3 and SHANK1. They also measured low micromolar affinity for the PDZ domain of SNX27, which is involved in retrograde transport from the endosome to the plasma membrane. Although plausible, whether or not NHERF3 and SNX27 are PDZ domain-containing

proteins interacting with ACE2 is an open question that will require follow-up experiments in the cell.

Tyr⁷⁸¹ in the ACE2 tail creates a potential multiway molecular switch regulated via phosphorylation

The tyrosine at residue 781 in ACE2 is a part of the motif patterns for four of the motifs listed above (Fig. 3 and Table 1) but must be phosphorylated to act as an SH2-binding motif. We searched the ACE2-related literature for reports of phosphorylation but were unable to find any with strong site identification. Examination of the human ACE2 entry in the database PhosphoSitePlus (143) revealed that high-throughput (HTP) phosphoproteomic studies, but no low-throughput (LTP) studies, identify pTyr⁷⁸¹. Thirteen HTP measurements identified phosphorylation at Tyr⁷⁸¹, and this residue is the only ACE2 phosphosite that is reproducible across multiple HTP datasets (Fig. 4). For example, pTyr⁷⁸¹ was one of 318 unique phosphopeptides belonging to 215 proteins analyzed from an erlotinib-treated breast cancer cell line model (144). Therefore, this site fulfills the phosphorylation requirement to be an SH2-binding motif.

As outlined above, four candidate sequence motifs overlap in the region surrounding Tyr⁷⁸¹: the YxxPhi endocytic sorting signal (ELM:TRG_ENDOCYTIC_2), an SH2 motif that mediates binding to SFKs, an NPY I-BAR-binding motif (ELM:LIG_IBAR_NPY_1), and the LIR autophagy motif (ELM:LIG_LIR_Gen_1). While the YxxPhi, NPY, and LIR motifs require an unphosphorylated state of Tyr⁷⁸¹, the SH2 motif requires Tyr⁷⁸¹ phosphorylation, creating the opportunity for a multiway phospho-switch acting in this region of ACE2 that directs different steps of the SARS-CoV-2 infection cycle. In support of this proposal, Kliche *et al.* (48) confirmed that the ACE2-YxxPhi interaction is negatively regulated by phosphorylation and that binding to the FYN SH2 domain requires Tyr⁷⁸¹ phos-

phorylation. The relative affinities of the ACE2 tail binders, which is still to be fully established, will dictate the competition between the interactions and the functional output. Current results indicate that the phosphorylated ACE2 tail can reach low micromolar affinity for SFKs and that the unphosphorylated state can bind to the AP2 μ 2 subunit with moderate affinity, while physiologically relevant interactions with autophagy components and I-BAR domains are still to be demonstrated. The state of this switch could be controlled by protein localization and by tyrosine kinase activity involving SRC/Abl and other tyrosine kinases, which are known to have increased abundance during endosomal processes (115) and viral infection (18) including in coronaviruses (2, 25–27). Similar switches have been described before, as with the cytotoxic T lymphocyte-associated protein 4 (CTLA-4) receptors, where SRC tyrosine kinases dictate the binding preferences of overlapping YxxPhi and SH2-binding motifs. In the unphosphorylated state, endocytosis is favored, whereas T cell activation brings about Tyr phosphorylation, shutting down endosomal recycling and initiating signaling through the recruitment of SH2 domain-containing proteins (106, 145–148). The CagA effector from *Helicobacter pylori* provides an example of a multiway molecular phospho-switch, where the choice for senescence versus cell proliferation is dictated by the SH2 domain-containing protein that forms a complex with phosphorylated CagA (24). Additional regulation can create a temporal gradient of the phospho-signal: CagA leads to remodeling of the actin cytoskeleton through its sequential phosphorylation by tyrosine kinases. Initial phosphorylation by SRC creates a negative feedback loop that terminates SRC signaling through activation of the SRC inhibitor Csk in the early stages of infection, while phosphorylation by Abl kinases leads to concerted changes in the phosphorylation of actin-regulatory proteins that drive actin-cytoskeletal rearrangements at later time points of infection (149).

Angiotensin-converting enzyme 2

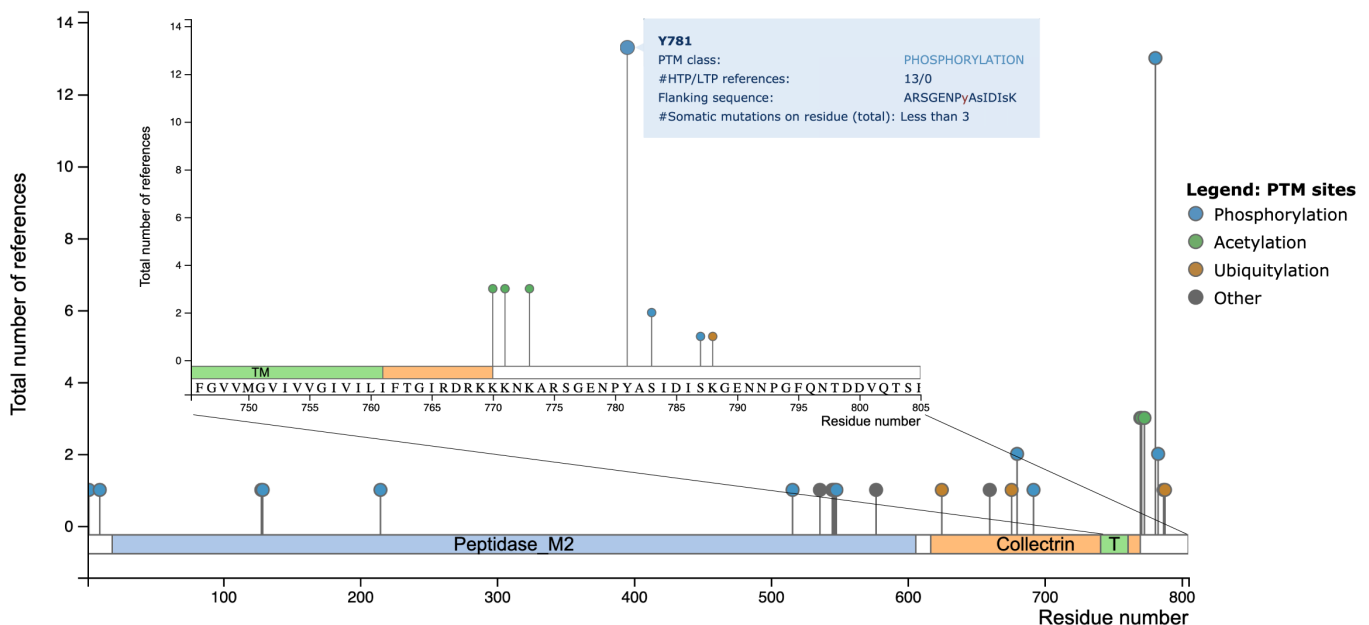


Fig. 4. The summary for the ACE2 C-terminal tail provided by PhosphoSitePlus. No low-throughput (LTP) studies have been recorded in the database for ACE2. Thirteen high-throughput (HTP) studies have identified phosphorylation on Tyr⁷⁸¹. Phosphosites reported in the extracellular part of ACE2 have only been reported once each and therefore are likely to be misidentified peptides.

A similar temporal regulation could be at play in SARS-CoV-2 endocytosis. This might be enacted by a Tyr⁷⁸¹ phospho-switch. The early attachment phase could be characterized by unphosphorylated Tyr⁷⁸¹ that allows the YxxPhi and NPY motifs to be active. During this phase, the YxxPhi motif could initiate RME by binding the AP2 complex μ 2 subunit, recruiting clathrin and other endocytic components to the viral attachment sites. In addition, some viruses can “surf” along filopodia by myosin-mediated actin cytoskeleton movements that transport the viral particles to the entry sites at the cell body, ultimately increasing their entry rate (125). The formation of these membrane protrusions could be promoted by the I-BAR-binding NPY motif. The relative affinity and availability of binders might dictate the sequential or concerted use of the YxxPhi and NPY motifs during the initial stage. Following the initial steps of membrane attachment and clathrin coat formation, actin polymerization is required to internalize the endocytic vesicles. This second step could be brought about by SFK-mediated Tyr⁷⁸¹ phosphorylation that leads to disengagement of the AP2 μ 2 subunit and I-BAR-containing proteins and to activation of actin-regulatory proteins through SFK recruitment. SRC and Abl, two of the SFKs predicted to bind the SH2 motif, are known to promote RME and actin cytoskeletal rearrangements (113, 115).

An alternative scenario that is not mutually exclusive with temporal regulation might be enabled by the multimeric nature of the spike protein and by attachment of several viral particles to a membrane domain, leading to adjacent ACE2 tails on the intracellular side that expose both phosphorylated and unphosphorylated motifs, allowing these three signaling steps to take place simultaneously. The separation between the RBD-binding sites in the ACE2 dimer is 68 Å calculated from PDB:6m17 (57), in close agreement with the distance between RBDs in the up conformation (~66 Å) measured from PDB: 6x2b (61) (fig. S1). While the outward orientation of the RBD-binding sites in ACE2 might preclude stable contacts between two RBDs and an ACE2 dimer, the spatial proximity implies that both ACE2 subunits are likely activated by the dynamic interaction of a spike protein trimer with an ACE2 dimer. The presence of several parallel routes for the recruitment of cytoskeleton components involving the NPY and SH2 motifs could provide the robustness needed to ensure the actin reorganization required for the uptake of virus-containing vesicles into the cytosol. Following endocytosis and fusion, viral components are released into the cell and viral replication takes place. SFKs have been shown to be inactive at the endosomal compartments, which would lead to dephosphorylation of Tyr⁷⁸¹ following endocytosis (115). During this phase, the last component of the switch could come into play, when the ACE2 protein that remains bound to spike protein-coated membranes could promote the hijack of autophagy components necessary to assemble the viral replication factories. However, the functionality of the LIR motif has not yet been established and might require other PTMs of the ACE2 tail, as suggested by Kliche *et al.* (48).

Known and candidate motifs in the β -integrin tails

Integrin β tails are short cytosolic C-terminal intrinsically disordered regions, similar to the analyzed region of ACE2. The three most probable integrin β subunit candidates at play in SARS-CoV-2 viral entry are β 3, β 6, and β 1. The C-terminal tails of all three subunits share a high degree of sequence similarity (with β 3 and β 6 being almost identical) and, similarly to ACE2, contain several known and candidate SLiMs (Table 1 and Fig. 5, A and B) that

propagate signals in the cytoplasm and regulate integrin activity not only through intracellular pathways but also changing the structural state of the ectodomains determining ligand-binding capacity (150). In addition, all three integrin β tails are very highly conserved (figs. S4 to S6), hinting at their high functional importance.

Integrin β tails contain a highly charged patch in their membrane-proximal region (Fig. 5A). This region is indispensable for the interaction between integrins and tyrosine kinases, including the SRC kinase Fyn (151) and FAK, most probably via the direct interaction with paxillin (152). Through these interactions, integrins regulate cytoskeletal remodeling (153) and the promotion of cell survival (154), as well as regulation of FA assembly and cell protrusion formation (155). In turn, FAK regulates integrin recycling and endosomal trafficking (156, 157).

Now, there is no consensus sequence motif describing these interactions, although a definition of HDR[KR]E has been proposed (158), matching integrins β 1, β 3, β 5, and β 6. This motif is under heavy regulation by several mechanisms. First, the interaction with tyrosine kinases seems to involve additional residues N-terminal of the charged motif core—most notably, the conserved lysine preceding the hydrophobic patch (159)—that are only accessible in the active state of the integrin dimer, as these regions are buried in the membrane otherwise (160). Second, the D residue of the motif forms a salt bridge with the cytosolic tail of the α subunit of the integrin in the inactive conformation of the receptor. Thus, this motif region is dependent on integrin activation regulated by ligand binding and intracellular interactions mediated by the downstream NPxY motifs.

The tails of integrins β 1, β 3, and β 6 contain two regions that match the apoPTB motif (Table 1 and Fig. 5A) as either NPxY (with two matches in integrin β 1 and 1-1 matches in integrins β 3 and β 6) or ϕ xNxxY (with 1-1 matches in integrins β 3 and β 6). Furthermore, these regions are known to have Tyr phosphorylation, matching the phosphorylated motif definition as well (ELM:LIG_PT_B_Phospho_1). These regions are known to be able to form β -turns and are recognition sites for PTB domains. In addition, NPxY motifs are the major sorting signals mediating interactions with FERM domains for regulating endosomal trafficking (161). In β -integrin tails, these motifs recruit adaptor proteins and clathrin, serving as sorting signals (162), and the NPxY motifs in the β 1 tail have a direct connection to viral entry for reovirus (163).

The NPxY motif switches mediate several interactions. The membrane-proximal NPxY motif binds talin-1, serving as a connection between the plasma membrane and the major cytoskeletal structures (164). Considering the expression profiles of talins, the most likely interaction partner of lung-expressed integrins is talin-1. Talin-1 contains a FERM domain, similarly to Ezrin, which establishes a direct interaction with the SARS-CoV spike protein upon viral fusion (126). However, the interaction between the RBD and integrins offers the virus an earlier point of interference with the cytoskeletal system, being able to modulate it cooperatively with the ACE2 actin-regulatory elements (NPY and SH2 motifs) before and during cellular entry. The talin/integrin interaction, however, presents a feedback loop: The binding of talin on the cytoplasmic side induces a structural rearrangement on the ectodomains of integrins, enabling a higher affinity interaction with RGD motif-containing ligands (165).

The membrane-proximal NPxY motif is also a binding site for docking protein 1 (DOK1), a negative regulator of integrin activation. DOK1 is in direct competition with talin for binding integrins (165). The competition is fundamentally influenced by phosphorylation

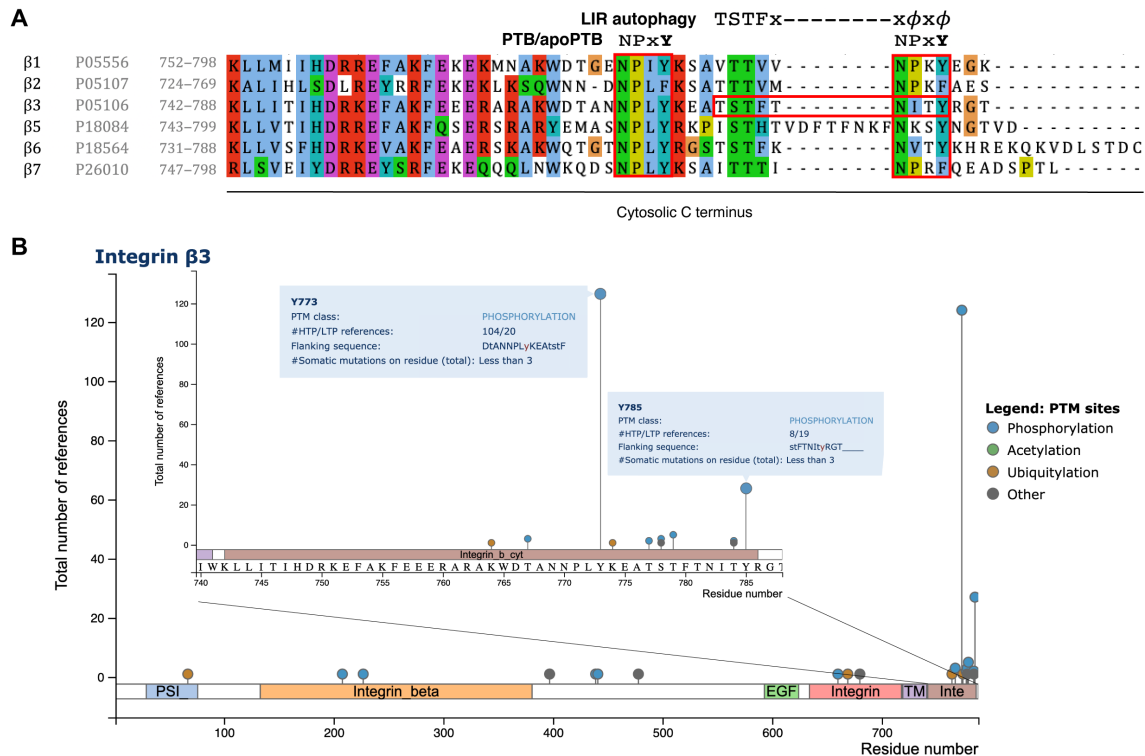


Fig. 5. Alignment of human integrins illustrating conserved motifs in the cytosolic C-terminal tail. (A) Multiple sequence alignment of human integrin C-terminal regions, not including the two most divergent β tails (β4 and β8). The alignment shows motif conservation of the NPxY and LIR motifs (key residues displayed above). Red boxes mark the conservation range of the PTB motif in all sequences and the location of the LIR motif in integrin β3. Protein names, UniProt IDs, and sequence numberings are listed on the left side of the alignment. **(B)** Summary of the PTMs on the C-terminal tail of integrin β3. Details of the experimental evidence for the PTB tyrosine phosphorylations are highlighted: pTyr⁷⁷³ (pY773) and pTyr⁷⁸⁵ (pY785). Graph was obtained from PhosphoSitePlus.

on Tyr⁷⁸³ (for integrin β1; fig. S7A), Tyr⁷⁷³ (for integrin β3; Fig. 5B), and Tyr⁷⁶² (for integrin β6; fig. S7B) of the NPxY motif. The unphosphorylated motif has a higher affinity toward talin, whereas phosphorylation prefers DOK1 (166); thus, the tyrosine acts as a phospho-switch regulating integrin activation.

The membrane-proximal NPxY motif also presents a binding site for a largely phosphorylation-independent interaction with the integrin cytoplasmic domain-associated protein-1 (ICAP-1). ICAP-1 is a fundamental regulator of the assembly of FAs and ICAP-1 knockdown reduced FA assembly (167), possibly working in conjunction with the membrane-proximal charged region. ICAP-1 seems to be specific for β1, and hence, the therapeutic considerations for targeting this pathway require the verification of the type of integrins expressed on AT2 cells (and other related cell types).

The membrane distal NPxY motif is a binding site for the FERM domain of kindlin (168). This interaction requires the integrin tail to be nonphosphorylated, and phosphorylation on Tyr⁷⁹⁵ (for integrin β1) or Tyr⁷⁸⁵ (for integrin β3) can switch off the interaction with kindlin-2 (169) (no corresponding Tyr phosphorylation has been identified in β6 tails as of yet). Kindlin binding (together with talin binding) is a crucial step in integrin activation and hence regulates the availability of integrins for extracellular ligands (170) and was also suggested to play a role in TGF-β1 signaling (171).

The two NPxY(-like) motifs in the integrin β tails not only constitute two separate phospho-switches (Fig. 5, fig. S7, and Table 1) but also act in synergy to give rise to more complex regulation. Filamin

and the PTB domain region of Shc1 each bind to both NPxY motifs (172, 173). Shc is an adaptor protein playing a key role in mitogen-activated protein kinase (MAPK) and Ras signaling pathways, and its interaction with integrin β3 requires both phosphorylations on Tyr⁷⁷³ and Tyr⁷⁸⁵ (172, 174). In contrast, binding of the immunoglobulin domain of filamin-A requires both tyrosines to be in a non-phosphorylated state. The filamin-A interaction can be considered as a main shutdown switch in integrin signaling, as this interaction induces the closed conformation of the integrin ectodomains, decreasing the chance of ligand binding (173). In addition, binding partners using both NPxY motifs may also serve as stronger modulators of endosomal trafficking, switching on enhanced signals.

Integrins are known to be connected to autophagy regulation, and therefore, motif identification and analysis might help suggest possible underlying molecular mechanisms. The connection between autophagy and cell adhesion has already been described, showing that both reduced FAK signaling (175) and detachment from the extracellular matrix via integrins (176) enhance autophagy. Atg-deficient cells have enhanced migration properties, and at the molecular level, there seems to be a direct connection between Atg proteins and integrins as well: autophagy stimulation increases the colocalization of β1 integrin-containing vesicles with LC3-stained autophagic vacuoles, whereas autophagy inhibition decreases the degradation of internalized β1 integrins (177). In *Drosophila* cells, it has been shown that the Wiskott-Aldrich syndrome protein and SCAR homolog (WASH) plays a connecting role between integrin

recycling and the efficiency of phagocytic and autophagic clearance (178). However, molecular details about how this connection is brought about are unclear.

Sequence analysis of integrin $\beta 3$ and $\beta 6$ tails shows a potential Atg-targeting LIR motif (Fig. 5A), similarly to the ACE2 tail. However, neither β -integrin tails conform to the regular expression introduced in earlier sections, as the hydrophobic residue following the core motif is a tyrosine (Tyr⁷⁸⁵ for $\beta 3$ and Tyr⁷⁷⁴ for $\beta 6$). Thus, to capture this instance as well, the regular expression needs to be modified to [EDST].[0,2][WFY][^RKP][^PG][ILMV].[0,4][LIVFMY]. LTP phosphorylation assays have determined that both Tyr⁷⁷³ and Tyr⁷⁸⁵ for $\beta 3$ are phosphorylated in live cells (Fig. 5B). However, such assays have also determined additional phosphorylation sites in the $\beta 3$ tail, Thr⁷⁷⁷, Ser⁷⁷⁸, Thr⁷⁷⁹, and Thr⁷⁸⁴. These phosphorylations are not connected to the NPxY motif switches in any known way but could serve as charge-based switches for the LIR motif. The peptide binding assays presented in the accompanying paper by Kliche *et al.* (48) show that phosphorylations introduced in the N-terminal tandem sites yielded low micromolar binding affinities. In addition, phosphorylation of Tyr⁷⁸⁵ further increases affinity, showing that the loss of the favorable interaction mediated by the C-terminal hydrophobic residue can be well compensated for by electrostatic interactions. While the current motif definition does not exactly fit the $\beta 1$ tail, there are also LTP phosphorylation assay data (179) for the existence of these phosphorylations in the corresponding residues, hinting at the possibility of the presence of a slightly modified motif. For $\beta 3$, as well as for $\beta 1$ and $\beta 6$ tails, the phosphorylation provides the negative charge required upstream of the FxxIxY LIR motif hydrophobic core. Phosphopeptides spanning the candidate region should also reveal whether the LIR motif-like region is a functional Atg-binding site in integrin $\beta 1$. Such experiments can also shed light on the existence of a rheostat-like behavior of multi-phosphorylation, already demonstrated to a certain extent for the $\beta 3$ LIR. The motif found in integrin $\beta 3$ is also present in integrin $\beta 2$, and the motif candidate identified in integrin $\beta 1$ is also present in integrin $\beta 6$.

Potential synergy between the ACE2 and integrin intracellular motifs

Bringing together the candidate SLiMs identified in the integrin β and ACE2 tails potentially strengthens the functional links between them and provides an emergent picture of SLiM-driven cooperative switches driving viral attachment, entry, and replication (Fig. 6). Following attachment of the spike protein to the receptors, the two NPxY motifs in the integrin subunit could act cooperatively with the apoPTB and YxxPhi motifs in ACE2 as sorting signals that mediate the internalization of viral particles into endosomes. The presence of several endocytic motifs in close proximity would strengthen the interaction with the endocytosis apparatus, creating a high-avidity environment for recruitment of RME components (107). During this time, the phosphorylated integrin NPxY motifs would also reinforce viral attachment through inside-out signaling, stabilizing the integrin ectodomain in the open, high ligand affinity conformation. As discussed previously, RME also involves the recruitment of adaptor molecules that activate rearrangements of the actin cytoskeleton required for the internalization of the endocytic vesicle. At this stage, the NPY and SH2 motifs in ACE2 would recruit several molecules that mediate actin polymerization signaling, prominently I-BAR-containing proteins IRSp53 and IRTKS as well

as actin cytoskeleton regulators activated by SFKs. While most of this actin signaling would serve to allow viral entry, additional actin recruitment processes could occur following viral fusion, such as that initiated by the interaction between the spike protein and Ezrin. Last, at later stages of infection, both integrins and ACE2 might remain attached to virus-associated DMVs and other replication-competent membranes where the RTC assembles. At this stage, ACE2 and integrins might cooperatively mediate the recruitment of autophagy components such as LC3 through the LIR motifs located in the cytosolic tails of both molecules.

SLiMs and their potential therapeutic implications

The analysis of candidate SLiMs in ACE2 and integrins suggests that SARS-CoV-2 hijacks both receptors, co-opting their SLiMs to drive viral attachment, entry, and replication. This creates an opportunity for drugging these interactions, or the processes they control, through host-directed therapies (HDTs) to prevent viral entry. On the basis of the identified candidate interactions, we collected a list of potentially useful drugs (Table 2) together with ChEMBL accessions (180); several are already registered for clinical trials (181).

The RGD sequence is used by a large number of viruses for cell attachment, via integrins (13). RGD mimics have been developed as inhibitors of integrin–extracellular matrix protein interaction for a variety of diseases. A cyclic RGD peptide [c-RGDf(NMe)V, cilengitide] has been developed clinically for glioblastoma treatment and other cancers. It proved safe but did not enhance the survival benefit (182). SARS-CoV-2 has a unique RGD sequence in the vicinity of the ACE2 binding region of its spike protein. It has been proposed that integrins may have a potential role for infectivity (12). If so, RGD mimetics might be able to block the RGD-binding site(s) on target cells and block the attachment of the virus. Another application that has been suggested is bacterial sepsis (sepsis is also a dreaded complication in COVID-19 patients), and experimental evidence in animals is available (183). Cilengitide is relatively specific for integrin $\alpha v\beta 3$ but also active on $\alpha v\beta 5$, $\alpha v\beta 1$, $\alpha v\beta 6$, $\alpha v\beta 8$, $\alpha IIb\beta 3$, $\alpha 4\beta 1$, and $\alpha 5\beta 1$ (in decreasing order of activity). The antibody abituzumab (DI-17E6) is a pan- αv antibody, meaning it is also active against other αv integrins and, consequently, may be better suited for blocking virus entry. It has been clinically tested in several cancer indications (184, 185).

As discussed above, tyrosine kinase-mediated phosphorylation plays an important role in virus entry and maturation, and several tyrosine kinase inhibitors have entered the clinic and some show effects on viral infection in cell culture. For example, saracatinib, an SRC and Abl inhibitor that has completed several clinical trials, mainly targeting cancers, inhibited replication of different coronaviruses including MERS-CoV, SARS-CoV, and HCoV-229E in cell culture infection experiments (27). After internalization and endosomal trafficking, imatinib, an Abl inhibitor, prevented fusion of SARS-CoV and MERS-CoV virions at the endosomal membrane in infected cell culture experiments (25). Using the avian model virus IBV, imatinib and two other Abl inhibitors (GNF2 and GNF5) prevented the fusion of the spike protein to the membrane of the target cell as well as cell-cell fusion and syncytia formation (2). More recently, tyrphostin A9, a platelet-derived growth factor receptor (PDGFR) tyrosine kinase inhibitor, came out from an HTP screening using cytopathic effect as readout and also showed in vitro inhibitory capacity to transmissible gastroenteritis virus (TGEV), an alphacoronavirus that infects pigs (26). The authors also showed

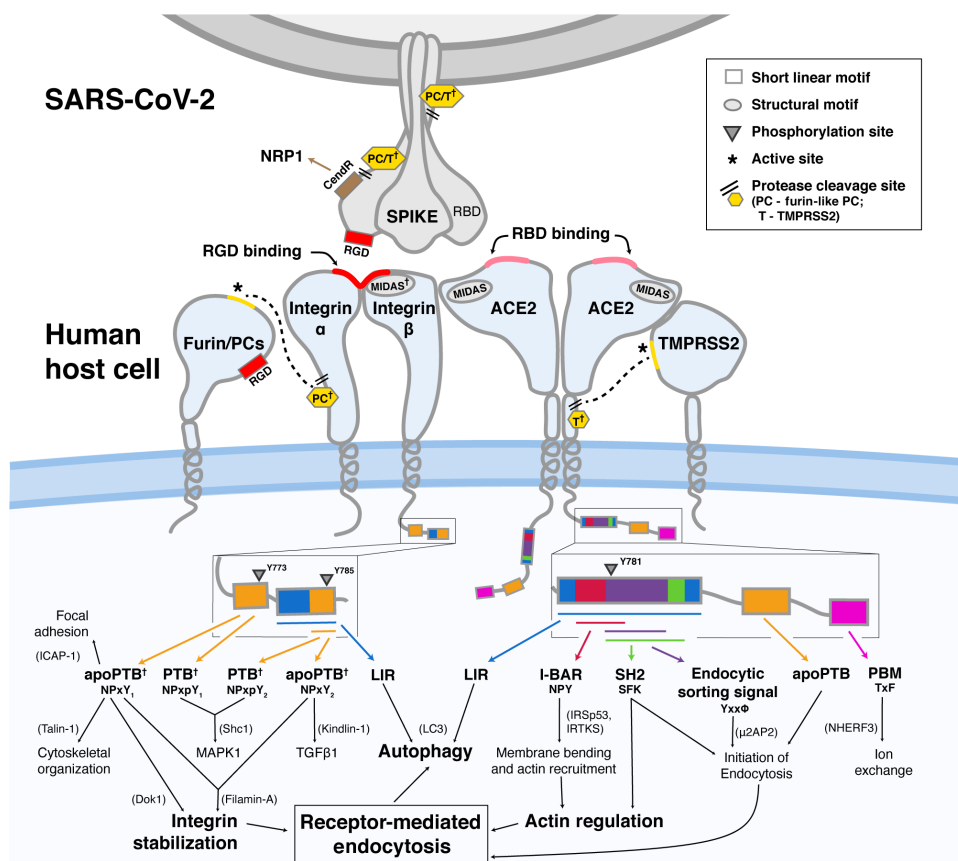


Fig. 6. Model of the proposed interplay between motifs in the interface between SARS-CoV-2 and a human host cell to achieve RME. Receptors of the SARS-CoV-2 (gray) and a human host cell (light blue) motifs involved in viral recognition and entry are shown in colored boxes. Elements shown in one of the monomers of a homotrimer (spike) or homodimer (ACE2) are also present in the other proteins forming that complex. Lines below motif boxes represent each of the overlapping motifs in that specific region. Arrows indicate the related cellular process, and the protein known to interact with their respective motif is indicated in parenthesis. Phosphorylation sites are shown as inverted triangles, with the respective sequence position indicated. For the β -integrin tail, the PTB/apoPTB phospho-switch is depicted as two separate versions of the same motif region, and the subscripts represent the motif order in the sequence. SLiMs mediating interactions are represented with boxes of different colors, protease cleavage sites with hexagons (PCs, furin-like proprotein convertases; T, TMPRSS2), phosphorylation sites with inverted triangles, and structural motifs with ovals. The color code is as follows: cleavage sites, yellow hexagon; apoPTB/PTB motif, orange; endocytic sorting signal motif, purple; I-BAR-binding motif, dark red; LIR motif, blue; MIDAS motif, gray; SH2 motif, green; PBM motif, magenta; RGD motif, bright red; and CendR motif, brown. † indicates that these motifs had been previously experimentally validated.

that tyrphostin A9 has a broad antiviral spectrum, being active against three other tested coronaviruses: MHV in murine L929 cells, porcine epidemic diarrhea virus in primate Vero cells, and feline infectious peritonitis virus in feline CCL-94 cells. The mode of action was found to be through p38 MAPK, at the post-adsorption stage. As FAK has been implicated in viral entry for other viruses including influenza A (186), experimental drugs targeting FAK, including some in clinical trials (187), can be considered for studying potential spike protein-induced integrin signaling. Now, 39 tyrosine kinase inhibitors are approved by the U.S. Food and Drug Administration (FDA): 11 target nonreceptor protein-tyrosine kinases and 28 inhibit receptor protein-tyrosine kinases (188). Consequently, tyrosine kinase inhibitors may be good candidates to test for their effect on SARS-CoV-2. For example, an inhibitor of the Abl and PDGFR kinases, flumatinib mesylate, showed 42% reduction of

SARS-CoV-2 infection of Vero E6 cells at 2.5 μ M (189). As part of the United Kingdom's ACCORD (Accelerating COVID-19 Research & Development) program, a clinical trial is underway to evaluate bemcentinib, a specific inhibitor of the receptor tyrosine kinase AXL in COVID-19 (190). AXL acts as a pleiotropic inhibitor of innate immunity (191) and is also a receptor for Ebola virus (192).

A number of protease inhibitors are now discussed for SARS-CoV-2 treatment. Serine protease inhibitor camostat mesylate is active against TMPRSS2 and blocks cell entry (4). Nafamostat mesylate—originally developed as a trypsin inhibitor (193)—also has been shown to inhibit TMPRSS2. Nafamostat mesylate is an approved anticoagulant in Japan, with clinical testing for COVID-19 infections now being conducted. The spike protein of SARS-CoV-2 contains a furin cleavage sequence (PRRARS|V). Consequently, furin convertase inhibitors are considered as antiviral agents (194). A prime example of such inhibitors is decanoyl-RVKR-CMK, which has been shown to inhibit cleavage of the SARS-CoV-2 spike protein at the S1/S2 site by furin (90). A large drug screen identified four drugs that targeted host cysteine proteases in SARS-CoV-2-infected human cells including VBY-825 (cathepsin B/L), ZLVG CHN2, ONO 5334 (cathepsin K), and MDL-28170 (cathepsin B and calpain I/II), with the latter two inhibiting SARS-CoV-2 replication in human induced pluripotent stem cell (iPSC) pneumocytes (189).

Many viruses enter the cell via endocytosis, and a number of candidate SLiMs relevant for SARS-CoV-2 infection are related to endocytosis (see above). Chlorpromazine, an antipsychotic dopamine D2 antagonist developed in the 1950s, is a potent endocytosis inhibitor (which likely explains its reputation as a “dirty drug” and some of its marked side effects, which can include low white blood cell levels). Like other tricyclic antipsychotics, the drug specifically inhibits the dynamin motor protein that is required to close off the endocytic vesicle at the plasma membrane (195). Anecdotally, it is thought that chlorpromazine (and presumably other tricyclic antipsychotics) might be protecting patients in psychiatric hospitals, and a clinical trial is now planned for COVID-19 (196). The potential use of endocytosis inhibitors such as amiodarone (197) and chlorpromazine in coronavirus infection is further discussed elsewhere (198). Another drug candidate, apilimod, acts later in the endosomal pathway by inhibiting the phosphoinositide kinase PIKfyve and blocks the SARS-CoV-2 entry pathway (38). Apilimod has been shown to strongly inhibit SARS-CoV-2 infection in two additional studies with the half-maximal inhibitory

concentration (IC_{50} ; 0.007 μ m) in human lung cells (199) and the half-maximal response (EC_{50} ; 0.023 μ m) in Vero E6 cells (189). Tyrphostin AG 538 (originally described as an inhibitor of insulin-like growth factor 1 receptor) is a preclinical inhibitor of the phosphoinositide kinase PI5P4K α (gene name PIP4K2A) (199) and showed 55% reduction of SARS-CoV-2 infection in Vero E6 cells (189). PIKfyve generates PtdIns5P, a regulatory phospholipid found on intracellular membrane systems including endosomes (201), whereas

PI5P4K α removes PtdIns5P by converting it to PtdIns(4, 5)P₂. Thus, apilimod and tyrphostin AG 538 might be targeting aspects of the same regulatory system controlling endosomal fates.

The threonine-specific AP2-associated protein kinase 1 (AAK1) phosphorylates the μ 2 subunit of the AP2 complex, promoting clathrin-mediated endocytosis (107). The related cyclin G-associated kinase (GAK) is also a regulator of endocytosis (202). It has been suggested that baricitinib, which is an AAK1 and GAK inhibitor in

Table 2. Drugs acting on various processes involved in viral entry and infection.

Name of drug	Mode of action	Clinical status	COVID19 ClinicalTrials.gov IDs*	Other details	ChEMBL ID [†]
Inhibitors of viral attachment					
Camostat mesylate	TMPRSS2 inhibition	Approved (Japan)	NCT04355052, NCT04374019, NCT04353284, NCT04321096, NCT04470544	Shown to be relevant in pancreatic fibrosis	590799
Nafamostat mesylate	TMPRSS2 inhibition	Approved (Japan)	NCT04473053	Also inhibits human tryptase. [‡] Has strong anticoagulant effect	3989553
Decanoyl-RVKR-CMK	Furin inhibition	Preclinical	–	Has been shown to inhibit CoV-2 spike cleavage at S1/S2 site by furin. [§] Because the NRP1 receptor binds after cleavage, furin inhibition is potentially more relevant	3126388
Abituzumab	Integrin inhibition (α v β 6, pan- α v)	Phase 2 in oncology	–	May also be relevant in fibrosis	2109621
Cilengitide	Integrin inhibition (α v β 3, α v β 5, α v β 6)	Phase 3 in oncology	–	May also be relevant in fibrosis, sepsis	429876
Suramin	Entry/early replication inhibitor, mode of action unknown	FDA approved	–	Drug of choice for treating African trypanosomiasis. Not without side effects	413376
Endocytosis inhibitors					
Amiodarone	Inhibits late endosomes	FDA approved	NCT04351763	Cell culture–based evidence for SARS-CoV inhibition	633
Chlorpromazine	Inhibits dynamin, thereby blocking clathrin-mediated endocytosis	FDA approved	NCT04354805, NCT04366739	Antipsychotic drug routinely used as endocytosis inhibitor in cell culture	823
Apilimod	Inhibits PIKfyve, a regulator of endosomal trafficking	Phase 2	NCT04446377	Blocks SARS-CoV-2 infection. Good safety profile from (failed) clinical trials for immune disease application. Clinical trials are registered	4297643
Imatinib	Abl inhibitor	FDA approved	NCT04422678, NCT04394416, NCT04346147, NCT04357613	First-line treatment for chronic myeloid leukemia	941
Teicoplanin	Inhibits cathepsin L (late endosomes and lysosome)	FDA approved	–	Glycopeptide antibiotic	2367892

continued on the next page

Name of drug	Mode of action	Clinical status	COVID19 ClinicalTrials.gov IDs*	Other details	ChEMBL ID [†]
Baricitinib	Inhibits AAK1 and GAK endocytic kinases	FDA approved	NCT04321993, NCT04340232, NCT04401579, NCT04362943, NCT04421027, NCT04390464, NCT04358614, NCT04346147, NCT04373044, NCT04393051, NCT04320277, NCT04399798	Also inhibits JAK kinase	2105759
BI-853520	FAK inhibitor	Phase 1	–	FAK has been implicated in the Influenza A virus cell entry and replication [¶]	3544961
Saracatinib	Src and Abl inhibitor	Phase 2 in oncology	–	Now also considered for Alzheimer's disease	217092
Tyrphostin A9	PDGF receptor kinase inhibitor (plus other activities)	Preclinical	–	Inhibits actin ring formation	78150
Autophagy modulators					
Metformin	NDUF modulation; mTOR pathway modulation (plus other activities?)	FDA approved	NCT04510194	Approved for type 2 diabetes	1431
Rapamycin Everolimus	mTORC1 inhibition	FDA approved	NCT04482712	Used for preventing transplant rejection	1908360413
Simvastatin	Autophagy up-regulation via mTOR	FDA approved	NCT04348695, NCT02735707	Treatment for dyslipidemia and atherosclerosis prevention	1064
Niclosamide Valinomycin (VAL)	Inhibits SKP2	Niclosamide—FDA approved; VAL—Preclinical	NCT04372082, NCT04436458, NCT04399356	Niclosamide—moderate effect; VAL targets MERS-CoV in cell culture, [§] known to inhibit SKP2	1448
NVP-BE2235/dactolisib	Autophagy induction	Phase 2	–	PI3k/Akt/mTOR	1879463
Spautin-1	Autophagy down-regulation by inhibition of USP10 and USP13	Preclinical	–	Inhibits dengue virus replication in tissue culture model.** Reported to have low toxicity in mice ^{††}	2391504
Fluoxetine	Affects endolysosomal acidification and cholesterol accumulation in the endosomes	FDA approved	NCT04377308	Used in treatment of major depressive disorder and obsessive compulsive disorder. Inhibits SARS-CoV-2 replication in Calu-3 and Vero E6 cells ^{‡‡}	41

*Clinical trial information can be checked by clicking the IDs (181). †Drug details are accessible by clicking ChEMBL IDs (180). ‡Reference (193). §Reference (90). ¶Reference (197). ¶¶Reference (186). #Reference (207). **Reference (205). ††Reference (204). ‡‡Reference (206).

addition to being a Janus kinase (JAK) inhibitor, be tested in COVID-19 (203).

The situation with targeting autophagy seems unclear. Autophagy activators might help the cell to consume incoming virus or speed up the establishment of the viral replication complexes and accelerate disease. Autophagy inhibitors might work in later stages of infec-

tion to dampen viral production, but this will depend on whether autophagy is active at the time or if the constituent components have been captured and effectively shut down. Several inhibitors/activators have been reported (a selection is listed in Table 2), which can target autophagy and multiple auxiliary signals feeding into the process of autophagy (204–207). One such axis is via the mTORC1

(mammalian target of rapamycin complex 1) complex. Active mTORC1 keeps the autophagy process inhibited by phosphorylating the ULK (Unc-51-like autophagy activating kinase) complex that is a key regulator in autophagy. Inhibition of mTORC1 activates autophagy. Multiple FDA-approved mTOR inhibitors are known and include rapamycin and everolimus. Rapamycin has been shown to be effective in cell culture for countering MERS-CoV infection (208) but has so far shown negative results in SARS-CoV-2 infection assays using Vero E6 cells (209), although the stage of infection might be crucial for the desired outcome. Simvastatin is another drug that is known to increase autophagy via the mTOR pathway (210). Simvastatin has also been reported to alleviate airway inflammation in a mouse asthma model (211). Another autophagy modulator is niclosamide that regulates autophagy by targeting the autophagy regulator Beclin1 via the SKP2 E3 ligase. In MERS-CoV infection, reduced Beclin1 levels lead to blocking fusion of autophagosomes and lysosomes and hence the virus protects itself in the host (43). Inhibiting SKP2 by niclosamide relieves Beclin1, allowing autophagosome-lysosome fusion and resumption of autophagy to reduce the MERS-CoV production. In addition, niclosamide (an FDA-approved drug for tapeworm infestations) and valinomycin (a naturally occurring antibiotic) have been shown to target SARS-CoV in cell cultures as well (207).

DISCUSSION

Examination of viral and cellular proteins that are known (or likely) to be involved in SARS-CoV-2 cell entry has proved a fruitful exercise in identifying multiple candidate SLiMs that might partake in the process. Because of the low sequence information content of SLiMs, it is difficult to get strong statistical support, and therefore, amino acid conservation over long evolutionary time periods is one of the most critical observations in this work. Experimental follow-up is essential before a SLiM can be considered to be functional. A first experimental step to indicate that these motifs might be functional is to test *in vitro* their ability to bind partner protein domains with an expected low micromolar or high nanomolar affinity, as is typical for SLiM interactions. In the case of PTB/apoPTB motif variants, it is difficult to do this quickly as the binding domain families are large and have not been systematically analyzed for motif preference, despite the known importance of this domain family in endocytosis and vesicle trafficking (136). However, in the accompanying experimental paper, Kliche *et al.* (48) were able to test peptide-domain binding for most of the newly predicted motifs in the ACE2 and integrin tails. Of those that could be quickly tested, several bound with plausible affinities, some were ambiguous, and some did not bind under the conditions of the experiments. Therefore, the ACE2 PBM, the SFK SH2-binding motif, the AP μ 2-binding motif, as well as the integrin β 3 phospho-LIR, are now available for their potential roles to be studied in cellular endocytic-autophagosome pathways both under normal conditions and when under pathogenic abuse.

Our observations of SLiM candidates in the viral entry system reveal previously unknown possible interactions mediating viral infection and reflect additional areas of the cell where drug repurposing for HDT might be explored. However, understanding the SARS-CoV-2 entry system has become more complicated and also more confusing. ACE2 is considered the canonical receptor for both SARS-CoV and SARS-CoV-2. Yet, the very rare expression of ACE2 in lungs implies that it cannot be the receptor underlying the severe lung pathology. Integrins are available to play this role and, as we have discussed, are

promising but not yet conclusively proven receptors. NRP1 has also been shown to be a SARS-CoV-2 receptor (91) and could also play a role in the lung disease. Like ACE2 and β integrins, we note that this newly identified receptor has a conserved apoPTB motif candidate and also a C-terminal SEA\$ motif that binds the PDZ domain of GIPC1 (212), an endocytosis adapter protein (fig. S8A). GIPC1 can also bind an SDA\$ motif in integrin α 5 (213). Integrins and NRP1 are involved in co-regulated signaling (text S1) and could therefore work together as SARS-CoV-2 receptors. The possibility of additional receptors should not be excluded. Earlier work with SARS-CoV has shown that several plasma membrane lectins can act as co-receptors (32), and in SARS-CoV-2, lectins expressed by innate immune cells bind the spike protein with high affinity and can promote viral entry (214). The cytosolic tails of a number of the lectin receptors are substrates of tyrosine kinases. Although tyrosine kinase inhibitors have frequently been shown to dampen pathogen invasion and disease progression in cell culture, there has been little effort to move these findings into the clinic (24). Because of their widespread use in cancer, the safety profiles of tyrosine kinase inhibitors are well known and we wonder whether this might be a neglected opportunity. COVID-19 might now drive the medical research forward: For example, in a small-scale trial, acalabrutinib, an inhibitor of BTK (Bruton's tyrosine kinase) that is an activator of macrophages, appears to be effective in dampening excessive inflammation in the lung of COVID-19 patients (215) and a larger trial is underway (190).

Drugging the cell to cure the pathogen using HDTs is unlikely to fully remove a virus. This would also be undesirable, because the immune system must mount a defense to prevent viral reinfection. Rather, dampening viral load during viral invasion or replication should be the target to give the host defenses time to respond. It is well known that drugs like Tamiflu, which slows influenza exit and therefore entry into uninfected cells, can only have a strong effect when taken prophylactically or early in infection (216). Depending on the importance of integrins in SARS-CoV-2 lung cell entry, given that it has become clear that ACE2 is barely expressed in the lung, altering virus-cell interactions is a possible role for cilengitide or other molecules that hamper integrin binding. An endocytosis inhibitor might play a similar role and is independent of receptor type. However, for any such inhibitor that passes the blood-brain barrier, effects on mood and other brain operations are an inevitable side effect: Even so, the endocytosis inhibitor chlorpromazine is a widely used drug with a well-known safety profile (217). AAK1 inhibition is also known to affect endocytosis, but there are no specific inhibitors in human trials, leading to the suggestion that the less specific JAK inhibitor baricitinib be tested (203).

Because of the presence of the cell attachment motif RGD in SARS-CoV-2, integrin inhibitors seem worthwhile to explore further. Cilengitide [a cyclic peptide that proved safe in patients but failed to show a survival benefit in glioblastoma (182)] is a relatively selective integrin α v β 3 and α v β 5 inhibitor, with low activity on various other integrins. It might be useful in two phases: It could block virus attachment to target cells, and it has also been proposed as a potential treatment in sepsis by preventing the attachment of bacteria to endothelial cells that can be RGD dependent (183). Sepsis was the most frequently observed complication among COVID-19 patients in Wuhan (218). Another potential application of integrin inhibitors, especially integrin α v β 6, would be lung fibrosis—patients on respirators tend to develop lung fibrosis and show increased α v β 6 levels (219). The antibody abrituzumab (DI-17E6) is a pan- α v antibody

with high potency on $\alpha v\beta 6$, i.e., also active against several αv integrins, and may consequently be better suited for blocking virus entry or may be suitable for lung fibrosis. It has been clinically tested in several cancer indications (184, 185), and proved safe, but did not achieve a survival benefit. Very recently, the integrin $\alpha v\beta 6$ inhibitor GSK3008348 has been shown to have an effect on lung fibrosis in a mouse therapeutic model (220).

The first large-scale proteomics study expressed 26 tagged SARS-CoV-2 proteins individually in human embryonic kidney (HEK) 293T cells, using affinity purification mass spectrometry to create a viral-human protein-protein interaction map and identified FDA-approved drugs, which were screened as inhibitors of these interactions (209). However, because this screen was not performed in the context of viral infection, it might have failed to reveal interactions essential for viral entry. The drug assays revealed positive results for inhibitors of mRNA translation and modulators of Sigma1/2 receptors and returned negative results for serine protease inhibitors (camostat and nafamostat), ACE inhibitors (captopril and lisinopril), mTOR inhibitors (rapamycin and sapanisertib), and a limited subset of tyrosine kinase inhibitors (midostaurin, ruxolitinib, and pazopanib). Translation and splicing regulators were further found as positive hits in another large-scale proteomics and transcriptome study (221). Another large drug screen using A549 lung cells identified AXL and AKT kinase inhibitors gilteritinib and ipatasertib and metalloproteinase inhibitors prinomastat and marimastat as promising drug candidates (222). A phosphoproteomic screen revealed that CK2, p38/MAPK, and cell cycle kinase pathways were regulated by SARS-CoV-2 infection, identifying kinase inhibitors that worked to inhibit viral replication. However, because tyrosine kinases were not strongly represented in the studied dataset (199), future work should help establish the role played by the tyrosine kinase signaling pathway in SARS-CoV-2 infection. While the positive hits in the latter studies provided useful targets for follow-up, the fact that the drug testing was performed in Vero E6 cells implies that negative results should be taken with caution until infection assays reflecting more physiological conditions are tested. A more recent large-scale drug screening found positive results for two tyrosine kinase inhibitors and confirmed strong inhibitory potency in lung iPSCs for two cysteine protease inhibitors and apilimod, with the latter also working in lung explant models (189). The three strongest inhibitors in this study affected viral entry, with apilimod showing potency comparable to that of remdesivir. This suggests that combination therapies using remdesivir together with apilimod or other kinase inhibitors depending on the infection stage might provide promising avenues for fighting COVID-19 infection.

In summary, we have presented evidence at the sequence level for SLiMs in ACE2 and β integrins with the potential to function in viral attachment, entry, and replication for SARS-CoV-2. We have identified several candidate molecular links and testable hypotheses that might help uncover the (still poorly understood) mechanisms of SARS-CoV-2 entry and replication. Because most of these motifs belong to host proteins acting as viral receptors, they are not revealed by virus-centered proteomic interaction assays. That they may well be functional, however, is indicated by sequence conservation, in some cases for hundreds of millions of years. In addition, the motifs are in appropriate cellular contexts to interact with their partner proteins. These putative motifs originally lacked direct experimental evidence, but the accompanying paper from Kliche *et al.* (48) shows that ACE2 YxxPhi, SH2, and PBM motifs and the integrin $\beta 3$

phospho-LIR bind to partner domains in vitro. Further experimental follow-up will yield insights into RME for the SARS-CoV-2 virus and, in addition, for the role of ACE2 in the normal cell, where it surely has much more functionality than its role as an ACE. Overall, the collection of candidate motifs in this system suggests that a range of HDTs might be explored including RGD inhibition, tyrosine kinase inhibition, endocytosis inhibition, and autophagy inhibition and/or activation.

MATERIALS AND METHODS

Protein sequences

Sequences of the spike protein, ACE2, and β integrins, together with homologous sequences, were retrieved from UniProt (222) (release 6 May 2020). The RatG spike protein sequence (Fig. 1) was retrieved from GenBank (224), and sequences of hagfish (*Eptatretus burgeri*) proteins were retrieved from UniParc (UniProt archive). All numberings defining regions in these proteins refer to the canonical sequences. RGD motif and its flanking region (2 amino acids) conservation were checked by using full-length high-quality spike protein sequences retrieved from the GISAID (53, 54) on 9 June 2020.

Identification of SLiMs

Candidate and known functional motifs were identified in the analyzed sequences using the ELM web server (23). The tail of ACE2 was also examined for SH2 predictions with ModPepInt server (116). Structural and context filters were used with their default settings. Motif candidates were manually inspected and were correlated with information from sequence conservation, available structures, and known phosphorylation sites, if applicable.

Protein alignments, structures, and abundance

Protein sequences were aligned using Clustal omega (225) using sequences extracted from UniProt and UniParc as inputs. Alignments were visualized using Jalview (226) and Clustal colors. The neighbor-joining tree in Fig. 1B was generated by Jalview with default parameters, and only the sequence regions shown in Fig. 1A were used. Protein structures were retrieved from the PDB (227) and were visualized using UCSF Chimera (228). Expression levels for various human proteins were taken from the Human Protein Atlas (81).

PTM sites

PTM sites in ACE2 and integrin $\beta 1$, $\beta 3$, and $\beta 6$ tails were taken from PhosphoSitePlus (v6.5.9.3) (143). Visualization of PTM data was done using the images generated by the PhosphoSitePlus web server using both HTP and LTP phosphorylation data.

SUPPLEMENTARY MATERIALS

stke.sciencemag.org/cgi/content/full/14/665/eabd0334/DC1

Text S1. Extended discussion on the potential of NRPs in SARS-CoV-2 cell entry.

Fig. S1. The structural feasibility of simultaneous integrin and ACE2 binding by SARS-CoV-2 spike protein trimers.

Fig. S2. Structural indication of a functional spike protein RBD:integrin $\alpha v\beta 6$ interaction.

Fig. S3. Alignment of human ACE2 transmembrane helix and C-terminal intracellular tail with homologous sequences of representative vertebrate collectrins from UniProt reference proteomes.

Fig. S4. Alignment of homologous sequences of integrin $\beta 3$ transmembrane helices and intracellular tails.

Fig. S5. Alignment of homologous sequences of integrin $\beta 1$ transmembrane helices and intracellular tails.

Fig. S6. Alignment of homologous sequences of integrin $\beta 6$ transmembrane helices and intracellular tails.

Fig. S7. PTMs in β -integrin tails.

Fig. S8. Transmembrane and intracellular regions of NRP1 and NRP2.

Table S1. SH2 domain specificity for the candidate ACE2 tail SH2 motif.

References (229–235)

[View/request a protocol for this paper from Bio-protocol.](#)

REFERENCES AND NOTES

- E. de Wit, N. van Doremalen, D. Falzarano, V. J. Munster, SARS and MERS: Recent insights into emerging coronaviruses. *Nat. Rev. Microbiol.* **14**, 523–534 (2016).
- J. M. Sisk, M. B. Frieman, C. E. Machamer, Coronavirus S protein-induced fusion is blocked prior to hemifusion by Abl kinase inhibitors. *J. Gen. Virol.* **99**, 619–630 (2018).
- W. Li, M. J. Moore, N. Vasiliieva, J. Sui, S. K. Wong, M. A. Berne, M. Somasundaran, J. L. Sullivan, K. Luzuriaga, T. C. Greenough, H. Choe, M. Farzan, Angiotensin-converting enzyme 2 is a functional receptor for the SARS coronavirus. *Nature* **426**, 450–454 (2003).
- M. Hoffmann, H. Kleine-Weber, S. Schroeder, N. Krüger, T. Herrler, S. Erichsen, T. S. Schiergens, G. Herrler, N.-H. Wu, A. Nitsche, M. A. Müller, C. Drosten, S. Pöhlmann, SARS-CoV-2 cell entry depends on ACE2 and TMPRSS2 and is blocked by a clinically proven protease inhibitor. *Cell* **181**, 271–280.e8 (2020).
- D. Wrapp, N. Wang, K. S. Corbett, J. A. Goldsmith, C.-L. Hsieh, O. Abiona, B. S. Graham, J. S. McLellan, Cryo-EM structure of the 2019-nCoV spike in the prefusion conformation. *Science* **367**, 1260–1263 (2020).
- Z. Zhou, X.-L. Yang, X.-G. Wang, B. Hu, L. Zhang, W. Zhang, H.-R. Si, Y. Zhu, B. Li, C.-L. Huang, H.-D. Chen, J. Chen, Y. Luo, H. Guo, R.-D. Jiang, M.-Q. Liu, Y. Chen, X.-R. Shen, X. Wang, X.-S. Zheng, K. Zhao, Q.-J. Chen, F. Deng, L.-L. Liu, B. Yan, F.-X. Zhan, Y.-Y. Wang, G.-F. Xiao, Z.-L. Shi, A pneumonia outbreak associated with a new coronavirus of probable bat origin. *Nature* **579**, 270–273 (2020).
- I. Hamming, W. Timens, M. L. C. Bulthuis, A. T. Lely, G. J. Navis, H. van Goor, Tissue distribution of ACE2 protein, the functional receptor for SARS coronavirus. A first step in understanding SARS pathogenesis. *J. Pathol.* **203**, 631–637 (2004).
- J. A. Aguiar, B. J.-M. Tremblay, M. J. Mansfield, O. Woody, B. Lobb, A. Banerjee, A. Chandiramohan, N. Tiessen, Q. Cao, A. Dvorkin-Gheva, S. Revill, M. S. Miller, C. Carlsten, L. Organ, C. Joseph, A. John, P. Hanson, R. Austin, B. M. McManus, G. Jenkins, K. Mossman, K. Ask, A. C. Doxey, J. A. Hirota, Gene expression and in situ protein profiling of candidate SARS-CoV-2 receptors in human airway epithelial cells and lung tissue. *Eur. Respir. J.* **56**, 2001123 (2020).
- L. Cantuti-Castelvetri, R. Ojha, L. D. Pedro, M. Djannatian, J. Franz, S. Kuivanen, F. van der Meer, K. Kallio, T. Kaya, M. Anastasina, T. Smura, L. Levanov, L. Szivovicza, A. Tobii, H. Kallio-Kokko, P. Österlund, M. Joensuu, F. A. Meunier, S. J. Butcher, M. S. Winkler, B. Mollenhauer, A. Helenius, O. Gokce, T. Teesalu, J. Hepojoki, O. Vapalahti, C. Stadelmann, G. Balistreri, M. Simons, Neuropilin-1 facilitates SARS-CoV-2 cell entry and infectivity. *Science* **370**, 856–860 (2020).
- F. Hikmet, L. Méar, Å. Edvinsson, P. Micke, M. Uhlén, C. Lindskog, The protein expression profile of ACE2 in human tissues. *Mol. Syst. Biol.* **16**, e9610 (2020).
- X. Zou, K. Chen, J. Zou, P. Han, J. Hao, Z. Han, Single-cell RNA-seq data analysis on the receptor ACE2 expression reveals the potential risk of different human organs vulnerable to 2019-nCoV infection. *Front. Med.* **14**, 185–192 (2020).
- C. J. Sigrist, A. Bridge, P. Le Mercier, A potential role for integrins in host cell entry by SARS-CoV-2. *Antiviral Res.* **177**, 104759 (2020).
- H. A. M. Hussein, L. R. Walker, U. M. Abdel-Raouf, S. A. Desouky, A. K. M. Montasser, S. M. Akula, Beyond RGD: Virus interactions with integrins. *Arch. Virol.* **160**, 2669–2681 (2015).
- P. L. Stewart, G. R. Nemerow, Cell integrins: Commonly used receptors for diverse viral pathogens. *Trends Microbiol.* **15**, 500–507 (2007).
- K. Triantafilou, Y. Takada, M. Triantafilou, Mechanisms of integrin-mediated virus attachment and internalization process. *Crit. Rev. Immunol.* **21**, 311–322 (2001).
- T. G. Kapp, F. Rechenmacher, S. Neubauer, O. V. Maltsev, E. A. Cavalcanti-Adam, R. Zarka, U. Reuning, J. Notni, H.-J. Wester, C. Mas-Moruno, J. Spatz, B. Geiger, H. Kessler, A comprehensive evaluation of the activity and selectivity profile of ligands for RGD-binding integrins. *Sci. Rep.* **7**, 39805 (2017).
- C. Guzzo, D. Ichikawa, C. Park, D. Phillips, Q. Liu, P. Zhang, A. Kwon, H. Miao, J. Lu, C. Rehm, J. Arthos, C. Cicala, M. S. Cohen, A. S. Fauci, J. H. Kehrl, P. Lusso, Virion incorporation of integrin $\alpha 4\beta 7$ facilitates HIV-1 infection and intestinal homing. *Sci. Immunol.* **2**, eaam7341 (2017).
- N. E. Davey, G. Travé, T. J. Gibson, How viruses hijack cell regulation. *Trends Biochem. Sci.* **36**, 159–169 (2011).
- K. Van Roey, H. Dinkel, R. J. Weatheritt, T. J. Gibson, N. E. Davey, The switches.ELM resource: A compendium of conditional regulatory interaction interfaces. *Sci. Signal.* **6**, rs7 (2013).
- K. Van Roey, T. J. Gibson, N. E. Davey, Motif switches: Decision-making in cell regulation. *Curr. Opin. Struct. Biol.* **22**, 378–385 (2012).
- T. J. Gibson, Cell regulation: Determined to signal discrete cooperation. *Trends Biochem. Sci.* **34**, 471–482 (2009).
- J. D. Scott, T. Pawson, Cell signaling in space and time: Where proteins come together and when they're apart. *Science* **326**, 1220–1224 (2009).
- M. Kumar, M. Gouwu, S. Michael, H. Sámano-Sánchez, R. Pansca, J. Glavina, A. Diakogianni, J. A. Valverde, D. Bukirova, J. Čalyševa, N. Palopoli, N. E. Davey, L. B. Chemes, T. J. Gibson, ELM—the eukaryotic linear motif resource in 2020. *Nucleic Acids Res.* **48**, D296–D306 (2020).
- H. Sámano-Sánchez, T. J. Gibson, Mimicry of short linear motifs by bacterial pathogens: A drugging opportunity. *Trends Biochem. Sci.* **45**, 526–544 (2020).
- C. M. Coleman, J. M. Sisk, R. M. Mingo, E. A. Nelson, J. M. White, M. B. Frieman, Abelson kinase inhibitors are potent inhibitors of severe acute respiratory syndrome coronavirus and middle east respiratory syndrome coronavirus fusion. *J. Virol.* **90**, 8924–8933 (2016).
- W. Dong, W. Xie, Y. Liu, B. Sui, H. Zhang, L. Liu, Y. Tan, X. Tong, Z. F. Fu, P. Yin, L. Fang, G. Peng, Receptor tyrosine kinase inhibitors block proliferation of TGEV mainly through p38 mitogen-activated protein kinase pathways. *Antiviral Res.* **173**, 104651 (2020).
- J. S. Shin, E. Jung, M. Kim, R. S. Baric, Y. Y. Go, Saracatinib inhibits Middle East respiratory syndrome-coronavirus replication in vitro. *Viruses* **10**, 283 (2018).
- V. Haucke, M. M. Kozlov, Membrane remodeling in clathrin-mediated endocytosis. *J. Cell Sci.* **131**, jcs216812 (2018).
- N. Kaksonen, A. Roux, Mechanisms of clathrin-mediated endocytosis. *Nat. Rev. Mol. Cell Biol.* **19**, 313–326 (2018).
- Y. Senju, P. Lappalainen, Regulation of actin dynamics by PI(4,5)P2 in cell migration and endocytosis. *Curr. Opin. Cell Biol.* **56**, 7–13 (2019).
- J. Grove, M. Marsh, The cell biology of receptor-mediated virus entry. *J. Cell Biol.* **195**, 1071–1082 (2011).
- C. A. M. de Haan, P. J. M. Rottier, Hosting the severe acute respiratory syndrome coronavirus: Specific cell factors required for infection. *Cell. Microbiol.* **8**, 1211–1218 (2006).
- I.-C. Huang, B. J. Bosch, F. Li, W. Li, K. H. Lee, S. Ghiran, N. Vasiliieva, T. S. Dermody, S. C. Harrison, P. R. Dormitzer, M. Farzan, P. J. M. Rottier, H. Choe, SARS coronavirus, but not human coronavirus NL63, utilizes cathepsin L to infect ACE2-expressing cells. *J. Biol. Chem.* **281**, 3198–3203 (2006).
- G. Simmons, J. D. Reeves, A. J. Rennekamp, S. M. Amberg, A. J. Piefer, P. Bates, Characterization of severe acute respiratory syndrome-associated coronavirus (SARS-CoV) spike glycoprotein-mediated viral entry. *Proc. Natl. Acad. Sci. U.S.A.* **101**, 4240–4245 (2004).
- S. Matsuyama, M. Ujike, S. Morikawa, M. Tashiro, F. Taguchi, Protease-mediated enhancement of severe acute respiratory syndrome coronavirus infection. *Proc. Natl. Acad. Sci. U.S.A.* **102**, 12543–12547 (2005).
- G. Simmons, D. N. Gosalia, A. J. Rennekamp, J. D. Reeves, S. L. Diamond, P. Bates, Inhibitors of cathepsin L prevent severe acute respiratory syndrome coronavirus entry. *Proc. Natl. Acad. Sci. U.S.A.* **102**, 11876–11881 (2005).
- A. H. de Wilde, E. J. Snijder, M. Kikkert, M. J. van Hemert, Host factors in coronavirus replication. *Curr. Top. Microbiol. Immunol.* **419**, 1–42 (2018).
- X. Ou, Y. Liu, X. Lei, P. Li, D. Mi, L. Ren, L. Guo, R. Guo, T. Chen, J. Hu, Z. Xiang, Z. Mu, X. Chen, J. Chen, K. Hu, Q. Jin, J. Wang, Z. Qian, Characterization of spike glycoprotein of SARS-CoV-2 on virus entry and its immune cross-reactivity with SARS-CoV. *Nat. Commun.* **11**, 1620 (2020).
- V. Deretic, B. Levine, Autophagy, immunity, and microbial adaptations. *Cell Host Microbe* **5**, 527–549 (2009).
- S. B. Kudchodkar, B. Levine, Viruses and autophagy. *Rev. Med. Virol.* **19**, 359–378 (2009).
- Y. Cong, P. Verlhac, F. Reggiori, The interaction between nidovirales and autophagy components. *Viruses* **9**, (2017).
- H. J. Maier, P. Britton, Involvement of autophagy in coronavirus replication. *Viruses* **4**, 3440–3451 (2012).
- N. C. Gassen, D. Niemeyer, D. Muth, V. M. Corman, S. Martinelli, A. Gassen, K. Hafner, J. Papies, K. Mösbauer, A. Zellner, A. S. Zannas, A. Herrmann, F. Holsboer, R. Brack-Werner, M. Boshart, B. Müller-Myhsok, C. Drosten, M. A. Müller, T. Rein, SKP2 attenuates autophagy through Beclin1-ubiquitination and its inhibition reduces MERS-Coronavirus infection. *Nat. Commun.* **10**, 5770 (2019).
- E. Prentice, W. G. Jerome, T. Yoshimori, N. Mizushima, M. R. Denison, Coronavirus replication complex formation utilizes components of cellular autophagy. *J. Biol. Chem.* **279**, 10136–10141 (2004).
- P. V'kovski, M. Gerber, J. Kelly, S. Pfaender, N. Ebert, S. Braga Lagache, C. Simillion, J. Portmann, H. Stalder, V. Gaschen, R. Bruggmann, M. H. Stoffel, M. Heller, R. Dijkman, V. Thiel, Determination of host proteins composing the microenvironment of coronavirus replicase complexes by proximity-labeling. *eLife* **8**, e42037 (2019).
- S. Klein, M. Cortese, S. L. Winter, M. Wachsmuth-Melm, C. J. Neufeldt, B. Cerikan, M. L. Stanifer, S. Boulant, R. Bartenschlager, P. Chlanda, SARS-CoV-2 structure and replication characterized by *in situ* cryo-electron tomography. *Nat. Commun.* **11**, 5885 (2020).
- F. Reggiori, I. Monastyrska, M. H. Verheije, T. Call, M. Ulasli, S. Bianchi, R. Bernasconi, C. A. M. de Haan, M. Molinari, Coronaviruses hijack the LC3-I-positive EDEMosomes,

- ER-derived vesicles exporting short-lived ERAD regulators, for replication. *Cell Host Microbe* **7**, 500–508 (2010).
48. J. Kliche, H. Kuss, M. A. Ali, Y. Ivarsson, Cytoplasmic short linear motifs in ACE2 and integrin $\beta 3$ link SARS-CoV-2 host cell receptors to mediators of endocytosis and autophagy. *Sci. Signal.* **14**, eabf1117 (2021).
 49. S. Su, G. Wong, W. Shi, J. Liu, A. C. K. Lai, J. Zhou, W. Liu, Y. Bi, G. F. Gao, Epidemiology, genetic recombination, and pathogenesis of coronaviruses. *Trends Microbiol.* **24**, 490–502 (2016).
 50. H. Minoux, C. Chipot, D. Brown, B. Maigret, Structural analysis of the KGD sequence loop of barbourin, an $\alpha 1 \text{Ib} \beta 3$ -specific disintegrin. *J. Comput. Aided Mol. Des.* **14**, 317–327 (2000).
 51. H. S. Selistre-de-Araujo, C. L. S. Pontes, C. F. Montenegro, A. C. B. M. Martin, Snake venom disintegrins and cell migration. *Toxins* **2**, 2606–2621 (2010).
 52. F. Curnis, R. Longhi, L. Crippa, A. Cattaneo, E. Dondossola, A. Bachi, A. Corti, Spontaneous formation of L-isoaspartate and gain of function in fibronectin. *J. Biol. Chem.* **281**, 36466–36476 (2006).
 53. S. Elbe, G. Buckland-Merrett, Data, disease and diplomacy: GISAID's innovative contribution to global health. *Glob. Chall.* **1**, 33–46 (2017).
 54. Y. Shu, J. McCauley, GISAID: Global initiative on sharing all influenza data—From vision to reality. *Euro Surveill.* **22**, 30494 (2017).
 55. W. S. J. Valdar, Scoring residue conservation. *Proteins* **48**, 227–241 (2002).
 56. A. C. Wang, Y.-J. Park, M. A. Tortorici, A. Wall, A. T. McGuire, D. Veasler, Structure, function, and antigenicity of the SARS-CoV-2 Spike glycoprotein. *Cell* **181**, 281–292.e6 (2020).
 57. R. Yan, Y. Zhang, Y. Li, L. Xia, Y. Guo, Q. Zhou, Structural basis for the recognition of SARS-CoV-2 by full-length human ACE2. *Science* **367**, 1444–1448 (2020).
 58. J. Lan, J. Ge, J. Yu, S. Shan, H. Zhou, S. Fan, Q. Zhang, X. Shi, Q. Wang, L. Zhang, X. Wang, Structure of the SARS-CoV-2 spike receptor-binding domain bound to the ACE2 receptor. *Nature* **581**, 215–220 (2020).
 59. Y. Watanabe, J. D. Allen, D. Wrapp, J. S. McLellan, M. Crispin, Site-specific glycan analysis of the SARS-CoV-2 spike. *Science* **369**, 330–333 (2020).
 60. N. E. Clarke, M. J. Fisher, K. E. Porter, D. W. Lambert, A. J. Turner, Angiotensin converting enzyme (ACE) and ACE2 bind integrins and ACE2 regulates integrin signalling. *PLOS ONE* **7**, e34747 (2012).
 61. R. Henderson, R. J. Edwards, K. Mansouri, K. Janowska, V. Stalls, S. Gobeil, M. Kopp, A. Hsu, M. Borgnia, R. Parks, B. F. Haynes, P. Acharya, Controlling the SARS-CoV-2 spike glycoprotein conformation. *Nat. Struct. Mol. Biol.* **27**, 925–933 (2020).
 62. D. Kiyozumi, M. Takeichi, I. Nakano, Y. Sato, T. Fukuda, K. Sekiguchi, Basement membrane assembly of the integrin $\alpha 8 \beta 1$ ligand nephronection requires Fraser syndrome-associated proteins. *J. Cell Biol.* **197**, 677–689 (2012).
 63. B. Pilecki, A. Schlosser, H. Wulf-Johansson, T. Trian, J. B. Moeller, N. Marcussen, J. A. Aguilar-Pimentel, M. H. de Angelis, J. Vestbo, P. Berger, U. Holmskov, G. L. Sorensen, Microfibrillar-associated protein 4 modulates airway smooth muscle cell phenotype in experimental asthma. *Thorax* **70**, 862–872 (2015).
 64. F. Cavallé, E. Neau, M. Vouters, H. Bry-Gauillard, A. Colombel, J. Milliez, Y. Le Bouc, IGFBP-1 inhibits EGF mitogenic activity in cultured endometrial stromal cells. *Biochem. Biophys. Res. Commun.* **345**, 754–760 (2006).
 65. G. K. Wang, L. Hu, G. N. Fuller, W. Zhang, An interaction between insulin-like growth factor-binding protein 2 (IGFBP2) and integrin $\alpha 5$ is essential for IGFBP2-induced cell mobility. *J. Biol. Chem.* **281**, 14085–14091 (2006).
 66. M. Cescon, F. Gattazzo, P. Chen, P. Bonaldo, Collagen VI at a glance. *J. Cell Sci.* **128**, 3525–3531 (2015).
 67. S. Rattila, C. E. E. Dunk, M. Im, O. Grichenko, Y. Zhou, M. Yanez-Mo, S. M. Blois, K. M. Yamada, O. Erez, N. Gomez-Lopez, S. J. Lye, B. Hinz, R. Romero, M. Cohen, G. Dveksler, Interaction of pregnancy-specific glycoprotein 1 with integrin $\text{A}5 \beta 1$ is a modulator of extravillous trophoblast functions. *Cell* **8**, 1369 (2019).
 68. R. Sato-Nishiuchi, I. Nakano, A. Ozawa, Y. Sato, M. Takeichi, D. Kiyozumi, K. Yamazaki, T. Yasunaga, S. Futaki, K. Sekiguchi, Polydom/SVEP1 is a ligand for integrin $\alpha 9 \beta 1$. *J. Biol. Chem.* **287**, 25615–25630 (2012).
 69. D. K. Shanley, P. A. Kiely, K. Golla, S. Allen, K. Martin, R. T. O'Riordan, M. Ball, J. D. Aplin, B. B. Singer, N. Caplice, N. Moran, T. Moore, Pregnancy-specific glycoproteins bind integrin $\alpha 1 \text{Ib} \beta 3$ and inhibit the platelet-fibrinogen interaction. *PLOS ONE* **8**, e57491 (2013).
 70. B. Shen, K. Vardy, P. Hughes, A. Tasdogan, Z. Zhao, R. Yue, G. M. Crane, S. J. Morrison, Integrin $\alpha 11$ is an osteolectin receptor and is required for the maintenance of adult skeletal bone mass. *eLife* **8**, e42274 (2019).
 71. D. A. Tumbarello, J. Temple, J. D. Brenton, $\beta 3$ integrin modulates transforming growth factor beta induced (TGF β) function and paclitaxel response in ovarian cancer cells. *Mol. Cancer* **11**, 36 (2012).
 72. X. Dong, N. E. Hudson, C. Lu, T. A. Springer, Structural determinants of integrin β -subunit specificity for latent TGF- β . *Nat. Struct. Mol. Biol.* **21**, 1091–1096 (2014).
 73. A. Kotecha, Q. Wang, X. Dong, S. L. Ilca, M. Ondiviela, R. Zihe, J. Seago, B. Charleston, E. E. Fry, N. G. A. Abrescia, T. A. Springer, J. T. Huiskonen, D. I. Stuart, Rules of engagement between $\alpha \text{v} \beta 6$ integrin and foot-and-mouth disease virus. *Nat. Commun.* **8**, 15408 (2017).
 74. J. Jovanovic, J. Takagi, L. Choulier, N. G. A. Abrescia, D. I. Stuart, P. A. van der Merwe, H. J. Mardon, P. A. Handford, $\alpha \text{v} \beta 6$ is a novel receptor for human Fibrillin-1. *J. Biol. Chem.* **282**, 6743–6751 (2007).
 75. J. M. Pilewski, J. D. Latoche, S. M. Arcasoy, S. M. Albelda, Expression of integrin cell adhesion receptors during human airway epithelial repair in vivo. *Am. J. Physiol.* **273**, L256–L263 (1997).
 76. F. Caccavari, D. Valdembrì, C. Sandri, F. Bussolino, G. Serini, Integrin signaling and lung cancer. *Cell Adh. Migr.* **4**, 124–129 (2010).
 77. T. Nakamura, P. R. Lozano, Y. Ikeda, Y. Iwanaga, A. Hinek, S. Minamisawa, C.-F. Cheng, K. Kobuke, N. Dalton, Y. Takada, K. Tashiro, J. Ross, T. Honjo, K. R. Chien, Fibulin-5/DANCE is essential for elastogenesis in vivo. *Nature* **415**, 171–175 (2002).
 78. B. Singh, C. Fu, J. Bhattacharya, Vascular expression of the $\alpha \text{v} \beta 3$ -integrin in lung and other organs. *Am. J. Physiol. Lung Cell. Mol. Physiol.* **278**, L217–L226 (2000).
 79. C. M. Teoh, S. S. L. Tan, T. Tran, Integrins as therapeutic targets for respiratory diseases. *Curr. Mol. Med.* **15**, 714–734 (2015).
 80. X. H. Yao, T. Y. Li, Z. C. He, Y. F. Ping, H. W. Liu, S. C. Yu, H. M. Mou, L. H. Wang, H. R. Zhang, W. J. Fu, T. Luo, F. Liu, Q. N. Guo, C. Chen, H. L. Xiao, H. T. Guo, S. Lin, D. F. Xiang, Y. Shi, G. Q. Pan, Q. R. Li, X. Huang, Y. Cui, X. Z. Liu, W. Tang, P. F. Pan, X. Q. Huang, Y. Q. Ding, X. W. Bian, A pathological report of three COVID-19 cases by minimal invasive autopsies. *Zhonghua Bing Li Xue Za Zhi* **49**, 411–417 (2020).
 81. M. Uhlén, L. Fagerberg, B. M. Hallström, C. Lindskog, P. Oksvold, A. Mardinoglu, Å. Sivertsson, C. Kampf, E. Sjödésted, A. Asplund, I. Olsson, K. Edlund, E. Lundberg, S. Navani, C. A.-K. Szigyorio, J. Odeberg, D. Djureinovic, J. O. Tankan, S. Hober, T. Alm, P.-H. Edqvist, H. Berling, H. Tegel, J. Mulder, J. Rockberg, P. Nilsson, J. M. Schwenk, M. Hamsten, K. von Feilitzen, M. Forsberg, L. Persson, F. Johansson, M. Zwaehlen, G. von Heijne, J. Nielsen, F. Pontén, Tissue-based map of the human proteome. *Science* **347**, 1260419 (2015).
 82. J. O. Lee, P. Rieu, M. A. Arnaout, R. Liddington, Crystal structure of the A domain from the alpha subunit of integrin CR3 (CD11b/CD18). *Cell* **80**, 631–638 (1995).
 83. K. Zhang, J. Chen, The regulation of integrin function by divalent cations. *Cell Adh. Migr.* **6**, 20–29 (2012).
 84. M. Lehmann, V. Rigot, N. G. Seidah, J. Marvaldi, J. C. Lissitzky, Lack of integrin α -chain endoproteolytic cleavage in furin-deficient human colon adenocarcinoma cells LoVo. *Biochem. J.* **317**, 803–809 (1996).
 85. J. C. Lissitzky, J. Luis, J. S. Munzer, S. Benjannet, F. Parat, M. Chrétien, J. Marvaldi, N. G. Seidah, Endoproteolytic processing of integrin pro- α subunits involves the redundant function of furin and proprotein convertase (PC) 5A, but not paired basic amino acid converting enzyme (PACE) 4, PC5B or PC7. *Biochem. J.* **346** (pt. 1), 133–138 (2000).
 86. H. Lou, A. M. Smith, L. C. Coates, N. X. Cawley, Y. P. Loh, N. P. Birch, The transmembrane domain of the prohormone convertase PC3: A key motif for targeting to the regulated secretory pathway. *Mol. Cell. Endocrinol.* **267**, 17–25 (2007).
 87. J. Lussan, S. Benjannet, J. Hamelin, D. Savaria, M. Chrétien, N. G. Seidah, The integrity of the RRGD sequence of the proprotein convertase PC1 is critical for its zymogen and C-terminal processing and for its cellular trafficking. *Biochem. J.* **326**, 737–744 (1997).
 88. C. Rovère, J. Luis, J. C. Lissitzky, A. Basak, J. Marvaldi, M. Chrétien, N. G. Seidah, The RGD motif and the C-terminal segment of proprotein convertase 1 are critical for its cellular trafficking but not for its intracellular binding to integrin $\alpha 5 \beta 1$. *J. Biol. Chem.* **274**, 12461–12467 (1999).
 89. B. Coutard, C. Valle, X. de Lamballerie, B. Canard, N. G. Seidah, E. Decroly, The spike glycoprotein of the new coronavirus 2019-nCoV contains a furin-like cleavage site absent in CoV of the same clade. *Antiviral Res.* **176**, 104742 (2020).
 90. M. Hoffmann, H. Kleine-Weber, S. Pöhlmann, A multibasic cleavage site in the spike protein of SARS-CoV-2 is essential for infection of human lung cells. *Mol. Cell* **78**, 779–784.e5 (2020).
 91. J. L. Daly, B. Simonetti, K. Klein, K.-E. Chen, M. K. Williamson, C. Antón-Plágaro, D. K. Shoemark, L. Simón-Gracia, M. Bauer, R. Hollandi, U. F. Greber, P. Horvath, R. B. Sessions, A. Helenius, J. A. Hiscox, T. Teesalu, D. A. Matthews, A. D. Davidson, B. M. Collins, P. J. Cullen, Y. Yamauchi, Neuropilin-1 is a host factor for SARS-CoV-2 infection. *Science* **370**, 861–865 (2020).
 92. M. Fukasawa, A. Matsushita, M. Korc, Neuropilin-1 interacts with integrin beta1 and modulates pancreatic cancer cell growth, survival and invasion. *Cancer Biol. Ther.* **6**, 1173–1180 (2007).
 93. D. Valdembrì, P. T. Caswell, K. I. Anderson, J. P. Schwarz, I. König, E. Astanina, F. Caccavari, J. C. Norman, M. J. Humphries, F. Bussolino, G. Serini, Neuropilin-1/GIPC1 signaling regulates $\alpha 5 \beta 1$ integrin traffic and function in endothelial cells. *PLOS Biol.* **7**, e25 (2009).
 94. B. A. Appleton, P. Wu, J. Maloney, J. Yin, W.-C. Liang, S. Stawicki, K. Mortara, K. K. Bowman, J. M. Elliott, W. Desmarais, J. F. Bazan, A. Bagri, M. Tessier-Lavigne, A. W. Koch, Y. Wu, R. J. Watts, C. Wiesmann, Structural studies of neuropilin/antibody complexes provide insights into semaphorin and VEGF binding. *EMBO J.* **26**, 4902–4912 (2007).
 95. S. Y. Kim, W. Jin, A. Sood, D. W. Montgomery, O. C. Grant, M. M. Fuster, L. Fu, J. S. Dordick, R. J. Woods, F. Zhang, R. J. Linhardt, Characterization of heparin and severe acute

- respiratory syndrome-related coronavirus 2 (SARS-CoV-2) spike glycoprotein binding interactions. *Antiviral Res.* **181**, 104873 (2020).
96. C. J. Mycroft-West, D. Su, I. Pagani, T. R. Rudd, S. Elli, S. E. Guimond, G. Miller, M. C. Z. Meneghetti, H. B. Nader, Y. Li, Q. M. Nunes, P. Procter, N. Mancini, M. Clementi, A. Bisio, N. R. Forsyth, J. E. Turnbull, M. Guerrini, D. G. Fernig, E. Vicenzi, E. A. Yates, M. A. Lima, M. A. Skidmore, Heparin inhibits cellular invasion by SARS-CoV-2: Structural dependence of the interaction of the surface protein (spike) S1 receptor binding domain with heparin. *bioRxiv* 2020.04.28.066761 [Preprint]. 8 May 2020. <https://doi.org/10.1101/2020.04.28.066761>.
 97. A. Heurich, H. Hofmann-Winkler, S. Gierer, T. Liepold, O. Jahn, S. Pöhlmann, TMPRSS2 and ADAM17 cleave ACE2 differentially and only proteolysis by TMPRSS2 augments entry driven by the severe acute respiratory syndrome coronavirus spike protein. *J. Virol.* **88**, 1293–1307 (2014).
 98. A. Shulla, T. Heald-Sargent, G. Subramanya, J. Zhao, S. Perlman, T. Gallagher, A transmembrane serine protease is linked to the severe acute respiratory syndrome coronavirus receptor and activates virus entry. *J. Virol.* **85**, 873–882 (2011).
 99. N. Iwata-Yoshikawa, T. Okamura, Y. Shimizu, H. Hasegawa, M. Takeda, N. Nagata, TMPRSS2 contributes to virus spread and immunopathology in the airways of murine models after coronavirus infection. *J. Virol.* **93**, e01815-18 (2019).
 100. T. Meng, H. Cao, H. Zhang, Z. Kang, D. Xu, H. Gong, J. Wang, Z. Li, X. Cui, H. Xu, H. Wei, X. Pan, R. Zhu, J. Xiao, W. Zhou, L. Cheng, J. Liu, The insert sequence in SARS-CoV-2 enhances spike protein cleavage by TMPRSS. *bioRxiv* 2020.02.08.926006 [Preprint]. 16 February 2020. <https://doi.org/10.1101/2020.02.08.926006>.
 101. T. J. Gibson, H. Dinkel, K. Van Roey, F. Diella, Experimental detection of short regulatory motifs in eukaryotic proteins: Tips for good practice as well as for bad. *Cell Commun. Signal.* **13**, 42 (2015).
 102. S. M. Shimeld, P. C. J. Donoghue, Evolutionary crossroads in developmental biology: Cyclostomes (lamprey and hagfish). *Development* **139**, 2091–2099 (2012).
 103. S. El-Gebali, J. Mistry, A. Bateman, S. R. Eddy, A. Luciani, S. C. Potter, M. Qureshi, L. J. Richardson, G. A. Salazar, A. Smart, E. L. L. Sonhammer, L. Hirsh, L. Paladin, D. Piovesan, S. C. E. Tosatto, R. D. Finn, The Pfam protein families database in 2019. *Nucleic Acids Res.* **47**, D427–D432 (2019).
 104. A. L. Mitchell, T. K. Attwood, P. C. Babbitt, M. Blum, P. Bork, A. Bridge, S. D. Brown, H.-Y. Chang, S. El-Gebali, M. I. Fraser, J. Gough, D. R. Haft, H. Huang, I. Letunic, R. Lopez, A. Luciani, F. Madeira, A. Marchler-Bauer, H. Mi, D. A. Natale, M. Necci, G. Nuka, C. Orengo, A. P. Pandurangan, T. Paysan-Lafosse, S. Pesseat, S. C. Potter, M. A. Qureshi, N. D. Rawlings, N. Redaschi, L. J. Richardson, C. Rivoire, G. A. Salazar, A. Sangrador-Vegas, C. J. A. Sigrist, I. Sillitoe, G. G. Sutton, N. Thanki, P. D. Thomas, S. C. E. Tosatto, S.-Y. Yong, R. D. Finn, InterPro in 2019: Improving coverage, classification and access to protein sequence annotations. *Nucleic Acids Res.* **47**, D351–D360 (2019).
 105. T. S. Kemp, *The Origin and Evolution of Mammals* (Oxford Univ. Press, 2005).
 106. D. J. Owen, P. R. Evans, A structural explanation for the recognition of tyrosine-based endocytotic signals. *Science* **282**, 1327–1332 (1998).
 107. J. S. Bonifacino, L. M. Traub, Signals for sorting of transmembrane proteins to endosomes and lysosomes. *Annu. Rev. Biochem.* **72**, 395–447 (2003).
 108. M. Tinti, L. Kiemer, S. Costa, M. L. Miller, F. Sacco, J. V. Olsen, M. Carducci, S. Paoluzi, F. Langone, C. T. Workman, N. Blom, K. Machida, C. M. Thompson, M. Schutkowski, S. Brunak, M. Mann, B. J. Mayer, L. Castagnoli, G. Cesareni, The SH2 domain interaction landscape. *Cell Rep.* **3**, 1293–1305 (2013).
 109. B. A. Liu, K. Jablonowski, E. E. Shah, B. W. Engelmann, R. B. Jones, P. D. Nash, SH2 domains recognize contextual peptide sequence information to determine selectivity. *Mol. Cell. Proteomics* **9**, 2391–2404 (2010).
 110. T. Kaneko, H. Huang, B. Zhao, L. Li, H. Liu, C. K. Voss, C. Wu, M. R. Schiller, S.-C. Li, Loops govern SH2 domain specificity by controlling access to binding pockets. *Sci. Signal.* **3**, ra34 (2010).
 111. S. Frese, W.-D. Schubert, A. C. Findeis, T. Marquardt, Y. S. Roske, T. E. B. Stradal, D. W. Heinz, The phosphotyrosine peptide binding specificity of Nck1 and Nck2 Src homology 2 domains. *J. Biol. Chem.* **281**, 18236–18245 (2006).
 112. H. Huang, L. Li, C. Wu, D. Schibli, K. Colwill, S. Ma, C. Li, P. Roy, K. Ho, Z. Songyang, T. Pawson, Y. Gao, S.-C. Li, Defining the specificity space of the human SRC homology 2 domain. *Mol. Cell. Proteomics* **7**, 768–784 (2008).
 113. J. Colicelli, ABL tyrosine kinases: Evolution of function, regulation, and specificity. *Sci. Signal.* **3**, re6 (2010).
 114. S. Kabrawala, M. D. Zimmer, K. G. Campellone, WHIMP links the actin nucleation machinery to Src-family kinase signaling during protrusion and motility. *PLoS Genet.* **16**, e1008694 (2020).
 115. J. Reinecke, S. Caplan, Endocytosis and the Src family of non-receptor tyrosine kinases. *Biomol. Concepts* **5**, 143–155 (2014).
 116. K. Kundu, M. Mann, F. Costa, R. Backofen, MoDPeplnt: An interactive web server for prediction of modular domain-peptide interactions. *Bioinformatics* **30**, 2668–2669 (2014).
 117. K. G. Campellone, M. J. Brady, J. G. Alamares, D. C. Rowe, B. M. Skehan, D. J. Tipper, J. M. Leong, Enterohaemorrhagic Escherichia coli Tir requires a C-terminal 12-residue peptide to initiate EspF-mediated actin assembly and harbours N-terminal sequences that influence pedestal length. *Cell. Microbiol.* **8**, 1488–1503 (2006).
 118. J. C. de Groot, K. Schlüter, Y. Carius, C. Quedenau, D. Vingadassalom, J. Faix, S. M. Weiss, J. Reichelt, C. Standfuss-Gabisch, C. F. Lesser, J. M. Leong, D. W. Heinz, K. Büssow, T. E. B. Stradal, Structural basis for complex formation between human IRSp53 and the translocated intimin receptor Tir of enterohaemorrhagic E. coli. *Structure* **19**, 1294–1306 (2011).
 119. Z. Chen, Z. Shi, T. Baumgart, Regulation of membrane-shape transitions induced by I-BAR domains. *Biophys. J.* **109**, 298–307 (2015).
 120. C. Prévost, H. Zhao, J. Manzi, E. Lemichez, P. Lappalainen, A. Callan-Jones, P. Bassereau, IRSp53 senses negative membrane curvature and phase separates along membrane tubules. *Nat. Commun.* **6**, 8529 (2015).
 121. H. Zhao, A. Pykäläinen, P. Lappalainen, I-BAR domain proteins: Linking actin and plasma membrane dynamics. *Curr. Opin. Cell Biol.* **23**, 14–21 (2011).
 122. S. Ahmed, W. I. Goh, W. Bu, I-BAR domains, IRSp53 and filopodium formation. *Semin. Cell Dev. Biol.* **21**, 350–356 (2010).
 123. H.-C. Cheng, B. M. Skehan, K. G. Campellone, J. M. Leong, M. K. Rosen, Structural mechanism of WASP activation by the enterohaemorrhagic E. coli effector EspF(U). *Nature* **454**, 1009–1013 (2008).
 124. N. A. Sallee, G. M. Rivera, J. E. Dueber, D. Vasilescu, R. D. Mullins, B. J. Mayer, W. A. Lim, The pathogen protein EspF(U) hijacks actin polymerization using mimicry and multivalency. *Nature* **454**, 1005–1008 (2008).
 125. K. Chang, J. Baginski, S. F. Hassan, M. Volin, D. Shukla, V. Tiwari, Filopodia and viruses: An analysis of membrane processes in entry mechanisms. *Front. Microbiol.* **7**, 300 (2016).
 126. J. K. Millet, F. Kien, C.-Y. Cheung, Y.-L. Siu, W.-L. Chan, H. Li, H.-L. Leung, M. Jaume, R. Bruzzone, J. S. M. Peiris, R. M. Altmeyer, B. Nal, Ezrin interacts with the SARS coronavirus Spike protein and restrains infection at the entry stage. *PLOS ONE* **7**, e49566 (2012).
 127. H. S. Saleh, U. Merkel, K. J. Geissler, T. Sperka, A. Sechi, C. Breithaupt, H. Morrison, Properties of an ezrin mutant defective in F-actin binding. *J. Mol. Biol.* **385**, 1015–1031 (2009).
 128. F.-C. Tsai, A. Bertin, H. Bousquet, J. Manzi, Y. Senju, M.-C. Tsai, L. Picas, S. Miserey-Lenkei, P. Lappalainen, E. Lemichez, E. Coudrier, P. Bassereau, Ezrin enrichment on curved membranes requires a specific conformation or interaction with a curvature-sensitive partner. *eLife* **7**, (2018).
 129. E. M. Cottam, M. C. Whelband, T. Wileman, Coronavirus NSP6 restricts autophagosome expansion. *Autophagy* **10**, 1426–1441 (2014).
 130. T. S. Fung, D. X. Liu, Human Coronavirus: Host-pathogen interaction. *Annu. Rev. Microbiol.* **73**, 529–557 (2019).
 131. Å. B. Birgisdottir, T. Lamark, T. Johansen, The LIR motif—Crucial for selective autophagy. *J. Cell Sci.* **126**, 3237–3247 (2013).
 132. H. L. Olsvik, T. Lamark, K. Takagi, K. B. Larsen, G. Evjen, A. Øvervatn, T. Mizushima, T. Johansen, FYCO1 contains a C-terminally extended, LC3A/B-preferring LC3-interacting region (LIR) motif required for efficient maturation of autophagosomes during basal autophagy. *J. Biol. Chem.* **290**, 29361–29374 (2015).
 133. E. A. Alemu, T. Lamark, K. M. Torgersen, A. B. Birgisdottir, K. B. Larsen, A. Jain, H. Olsvik, A. Øvervatn, V. Kirkin, T. Johansen, ATG8 family proteins act as scaffolds for assembly of the ULK complex: Sequence requirements for LC3-interacting region (LIR) motifs. *J. Biol. Chem.* **287**, 39275–39290 (2012).
 134. M. S. Rasmussen, Å. B. Birgisdottir, T. Johansen, Use of peptide arrays for identification and characterization of LIR motifs. *Methods Mol. Biol.* **1880**, 149–161 (2019).
 135. M. M. Zhou, K. S. Ravichandran, E. F. Olejniczak, A. M. Petros, R. P. Meadows, M. Sattler, J. E. Harlan, W. S. Wade, S. J. Burakoff, S. W. Fesik, Structure and ligand recognition of the phosphotyrosine binding domain of Shc. *Nature* **378**, 584–592 (1995).
 136. M. T. Uhlik, B. Temple, S. Bencharit, A. J. Kimple, D. P. Siderovski, G. L. Johnson, Structural and evolutionary division of phosphotyrosine binding (PTB) domains. *J. Mol. Biol.* **345**, 1–20 (2005).
 137. A. Ernst, S. L. Sazinsky, S. Hui, B. Currell, M. Dharsee, S. Seshagiri, G. D. Bader, S. S. Sidhu, Rapid evolution of functional complexity in a domain family. *Sci. Signal.* **2**, ra50 (2009).
 138. G. P. Manjunath, P. L. Ramanujam, S. Galande, Structure function relations in PDZ-domain-containing proteins: Implications for protein networks in cellular signalling. *J. Biosci.* **43**, 155–171 (2018).
 139. N. R. Christensen, J. Čalyševa, E. F. A. Fernandes, S. Lüchow, L. S. Clemmensen, L. M. Haugaard-Kedström, K. Strömgaard, PDZ domains as drug targets. *Adv. Ther.* **2**, 1800143 (2019).
 140. A. Ernst, B. A. Appleton, Y. Ivarsson, Y. Zhang, D. Gfeller, C. Wiesmann, S. S. Sidhu, A structural portrait of the PDZ domain family. *J. Mol. Biol.* **426**, 3509–3519 (2014).
 141. S. M. Gisler, S. Pribanic, D. Bacic, P. Forrer, A. Gantenbein, L. A. Sabourin, A. Tsuji, Z.-S. Zhao, E. Manser, J. Biber, H. Murer, PDZK1: I. A major scaffold in brush borders of proximal tubular cells. *Kidney Int.* **64**, 1733–1745 (2003).

142. S. Srivastava, K. Nakagawa, X. He, T. Kimura, T. Fukutomi, S. Miyauchi, H. Sakurai, N. Anzai, Identification of the multivalent PDZ protein PDZK1 as a binding partner of sodium-coupled monocarboxylate transporter SMCT1 (SLC5A8) and SMCT2 (SLC5A12). *J. Physiol. Sci.* **69**, 399–408 (2019).
143. P. V. Hornbeck, J. M. Kornhauser, V. Latham, B. Murray, V. Nandhikonda, A. Nord, E. Skrzypek, T. Wheeler, B. Zhang, F. Gnad, 15 years of PhosphoSitePlus®: Integrating post-translationally modified sites, disease variants and isoforms. *Nucleic Acids Res.* **47**, D433–D441 (2019).
144. M. Tzouros, S. Golling, D. Avila, J. Lamerz, M. Berrera, M. Ebeling, H. Langen, A. Augustin, Development of a 5-plex SILAC method tuned for the quantitation of tyrosine phosphorylation dynamics. *Mol. Cell. Proteomics* **12**, 3339–3349 (2013).
145. J. D. Bradshaw, P. Lu, G. Leytze, J. Rodgers, G. L. Schieven, K. L. Bennett, P. S. Linsley, S. E. Kurtz, Interaction of the cytoplasmic tail of CTLA-4 (CD152) with a clathrin-associated protein is negatively regulated by tyrosine phosphorylation. *Biochemistry* **36**, 15975–15982 (1997).
146. S. Miyatake, C. Nakaseko, H. Umemori, T. Yamamoto, T. Saito, Src family tyrosine kinases associate with and phosphorylate CTLA-4 (CD152). *Biochem. Biophys. Res. Commun.* **249**, 444–448 (1998).
147. H. Ohno, M. C. Fournier, G. Poy, J. S. Bonifacio, Structural determinants of interaction of tyrosine-based sorting signals with the adaptor medium chains. *J. Biol. Chem.* **271**, 29009–29015 (1996).
148. T. Shiratori, S. Miyatake, H. Ohno, C. Nakaseko, K. Isono, J. S. Bonifacio, T. Saito, Tyrosine phosphorylation controls internalization of CTLA-4 by regulating its interaction with clathrin-associated adaptor complex AP-2. *Immunity* **6**, 583–589 (1997).
149. N. Tegtmeyer, S. Backert, Role of Abl and Src family kinases in actin-cytoskeletal rearrangements induced by the *Helicobacter pylori* CagA protein. *Eur. J. Cell Biol.* **90**, 880–890 (2011).
150. N. J. Anthis, I. D. Campbell, The tail of integrin activation. *Trends Biochem. Sci.* **36**, 191–198 (2011).
151. K. B. Reddy, D. M. Smith, E. F. Plow, Analysis of Fyn function in hemostasis and alphaIIb beta3-integrin signaling. *J. Cell Sci.* **121**, 1641–1648 (2008).
152. G. Liu, C. D. Guibao, J. Zheng, Structural insight into the mechanisms of targeting and signaling of focal adhesion kinase. *Mol. Cell. Biol.* **22**, 2751–2760 (2002).
153. Z. Lv, M. Hu, X. Ren, M. Fan, J. Zhen, L. Chen, J. Lin, N. Ding, Q. Wang, R. Wang, Fyn mediates high glucose-induced actin cytoskeleton reorganization of podocytes via promoting ROCK activation in vitro. *J. Diabetes Res.* **2016**, 5671803 (2016).
154. X. Tang, Y. Feng, K. Ye, Src-family tyrosine kinase fyn phosphorylates phosphatidylinositol 3-kinase enhancer-activating Akt, preventing its apoptotic cleavage and promoting cell survival. *Cell Death Differ.* **14**, 368–377 (2007).
155. Y.-L. Hu, S. Lu, K. W. Szeto, J. Sun, Y. Wang, J. C. Lasheras, S. Chien, FAK and paxillin dynamics at focal adhesions in the protrusions of migrating cells. *Sci. Rep.* **4**, 6024 (2014).
156. G. Mana, D. Valdembrí, G. Serini, Conformationally active integrin endocytosis and traffic: Why, where, when and how? *Biochem. Soc. Trans.* **48**, 83–93 (2020).
157. G. P. F. Nader, E. J. Ezratty, G. G. Gundersen, FAK, talin and PIPKly regulate endocytosed integrin activation to polarize focal adhesion assembly. *Nat. Cell Biol.* **18**, 491–503 (2016).
158. K. R. Legate, R. Fässler, Mechanisms that regulate adaptor binding to β -integrin cytoplasmic tails. *J. Cell Sci.* **122**, 187–198 (2009).
159. K. B. Reddy, P. Gascard, M. G. Price, E. V. Negrescu, J. E. Fox, Identification of an interaction between the m-band protein skelemin and β -Integrin subunits. Colocalization of a skelemin-like protein with β_1 - and β_3 -integrins in non-muscle cells. *J. Biol. Chem.* **273**, 35039–35047 (1998).
160. A. Stefansson, A. Armulik, I. Nilsson, G. von Heijne, S. Johansson, Determination of N- and C-terminal borders of the transmembrane domain of integrin subunits. *J. Biol. Chem.* **279**, 21200–21205 (2004).
161. R. Ghai, A. Bugarcic, H. Liu, S. J. Norwood, S. Skeldal, E. J. Coulson, S. S.-C. Li, R. D. Teasdale, B. M. Collins, Structural basis for endosomal trafficking of diverse transmembrane cargos by PX-FERM proteins. *Proc. Natl. Acad. Sci. U.S.A.* **110**, E643–E652 (2013).
162. H. Ohno, J. Stewart, M. C. Fournier, I. Rhee, S. Miyatake, T. Saito, A. Gallusser, T. Kirchhausen, J. S. Bonifacio, Interaction of tyrosine-based sorting signals with clathrin-associated proteins. *Science* **269**, 1872–1875 (1995).
163. M. S. Maginnis, B. A. Mainou, A. Derdowski, E. M. Johnson, R. Zent, T. S. Dermody, NPXY motifs in the beta1 integrin cytoplasmic tail are required for functional reovirus entry. *J. Virol.* **82**, 3181–3191 (2008).
164. A. Horwitz, K. Duggan, C. Buck, M. C. Beckerle, K. Burridge, Interaction of plasma membrane fibronectin receptor with talin—A transmembrane linkage. *Nature* **320**, 531–533 (1986).
165. S. Tadokoro, S. J. Shattil, K. Eto, V. Tai, R. C. Liddington, J. M. de Pereda, M. H. Ginsberg, D. A. Calderwood, Talin binding to integrin beta tails: A final common step in integrin activation. *Science* **302**, 103–106 (2003).
166. C. L. Oxley, N. J. Anthis, E. D. Lowe, I. Vakoniakis, I. D. Campbell, K. L. Wegener, An integrin phosphorylation switch: The effect of β_3 integrin tail phosphorylation on Dok1 and talin binding. *J. Biol. Chem.* **283**, 5420–5426 (2008).
167. B. Alvarez, P. J. M. Stroeken, M. J. Edel, E. Roos, Integrin cytoplasmic domain-associated protein-1 (ICAP-1) promotes migration of myoblasts and affects focal adhesions. *J. Cell. Physiol.* **214**, 474–482 (2008).
168. Y.-Q. Ma, J. Qin, C. Wu, E. F. Plow, Kindlin-2 (Mig-2): A co-activator of beta3 integrins. *J. Cell Biol.* **181**, 439–446 (2008).
169. K. Bledzka, K. Bialkowska, H. Nie, J. Qin, T. Byzova, C. Wu, E. F. Plow, Y.-Q. Ma, Tyrosine phosphorylation of integrin beta3 regulates kindlin-2 binding and integrin activation. *J. Biol. Chem.* **285**, 30370–30374 (2010).
170. C. Herz, M. Aumailley, C. Schulte, U. Schlötzer-Schrehardt, L. Bruckner-Tuderman, C. Has, Kindlin-1 is a phosphoprotein involved in regulation of polarity, proliferation, and motility of epidermal keratinocytes. *J. Biol. Chem.* **281**, 36082–36090 (2006).
171. S. Kloeker, M. B. Major, D. A. Calderwood, M. H. Ginsberg, D. A. Jones, M. C. Beckerle, The Kindler syndrome protein is regulated by transforming growth factor- β and involved in integrin-mediated adhesion. *J. Biol. Chem.* **279**, 6824–6833 (2004).
172. L. Deshmukh, V. Gorbatyuk, O. Vinogradova, Integrin β_3 phosphorylation dictates its complex with the Shc phosphotyrosine-binding (PTB) domain. *J. Biol. Chem.* **285**, 34875–34884 (2010).
173. J. Liu, M. Das, J. Yang, S. S. Ithychanda, V. P. Yakubenko, E. F. Plow, J. Qin, Structural mechanism of integrin inactivation by filamin. *Nat. Struct. Mol. Biol.* **22**, 383–389 (2015).
174. E. Audero, I. Cascone, F. Maniero, L. Napione, M. Arese, L. Lanfrancone, F. Bussolino, Adaptor ShcA protein binds tyrosine kinase Tie2 receptor and regulates migration and sprouting but not survival of endothelial cells. *J. Biol. Chem.* **279**, 13224–13233 (2004).
175. E. Sandilands, B. Serrels, D. G. McEwan, J. P. Morton, J. P. Macagno, K. McLeod, C. Stevens, V. G. Brunton, W. Y. Langdon, M. Vidal, O. J. Sansom, I. Dikic, S. Wilkinson, M. C. Frame, Autophagic targeting of Src promotes cancer cell survival following reduced FAK signalling. *Nat. Cell Biol.* **14**, 51–60 (2011).
176. A. Vlahakis, J. Debnath, The interconnections between autophagy and integrin-mediated cell adhesion. *J. Mol. Biol.* **429**, 515–530 (2017).
177. V. Tuloup-Minguez, A. Hamai, A. Greffard, V. Nicolas, P. Codogno, J. Botti, Autophagy modulates cell migration and β_1 integrin membrane recycling. *Cell Cycle* **12**, 3317–3328 (2013).
178. B. M. Nagel, M. Bechtold, L. G. Rodriguez, S. Bogdan, *Drosophila* WASH is required for integrin-mediated cell adhesion, cell motility and lysosomal neutralization. *J. Cell Sci.* **130**, 344–359 (2017).
179. K. Wennerberg, R. Fässler, B. Wärmegård, S. Johansson, Mutational analysis of the potential phosphorylation sites in the cytoplasmic domain of integrin beta1A. Requirement for threonines 788–789 in receptor activation. *J. Cell Sci.* **111**, 1117–1126 (1998).
180. D. Mendez, A. Gaulton, A. P. Bento, J. Chambers, M. De Veij, E. Félix, M. P. Magariños, J. F. Mosquera, P. Mutowo, M. Nowotka, M. Gordillo-Marañón, F. Hunter, L. Junco, G. Mugumbate, M. Rodriguez-Lopez, F. Atkinson, N. Bosc, C. J. Radoux, A. Segura-Cabrera, A. Hersey, A. R. Leach, ChEMBL: Towards direct deposition of bioassay data. *Nucleic Acids Res.* **47**, D930–D940 (2019).
181. D. A. Zarin, K. M. Fain, H. D. Dobbins, T. Tse, R. J. Williams, 10-year update on study results submitted to ClinicalTrials.gov. *N. Engl. J. Med.* **381**, 1966–1974 (2019).
182. R. Stupp, M. E. Hegi, T. Gorlia, S. C. Erridge, J. Perry, Y.-K. Hong, K. D. Aldape, B. Lhermitte, T. Pietsch, D. Grujcic, J. P. Steinbach, W. Wick, R. Tarnawski, D.-H. Nam, P. Hau, A. Weyerbrock, M. J. B. Taphoorn, C.-C. Shen, N. Rao, L. Thurzo, U. Herrlinger, T. Gupta, R.-D. Kortmann, K. Adamska, C. McBain, A. A. Brandes, J. C. Tonn, O. Schnell, T. Wiegell, C.-Y. Kim, L. B. Nabors, D. A. Reardon, M. J. van den Bent, C. Hicking, A. Markivskyy, M. Picard, M. Weller; European Organisation for Research and Treatment of Cancer (EORTC); Canadian Brain Tumor Consortium; CENTRIC study team, Cilengitide combined with standard treatment for patients with newly diagnosed glioblastoma with methylated MGMT promoter (CENTRIC EORTC 26071-22072 study): A multicentre, randomised, open-label, phase 3 trial. *Lancet Oncol.* **15**, 1100–1108 (2014).
183. C. D. Garciaarena, T. M. McHale, I. Martin-Loeches, S. W. Kerrigan, Pre-emptive and therapeutic value of blocking bacterial attachment to the endothelial alphaVbeta3 integrin with cilengitide in sepsis. *Crit. Care* **21**, 246 (2017).
184. E. Élez, I. Kocáková, T. Höhler, U. M. Martens, C. Bokemeyer, E. Van Cutsem, B. Melichar, M. Smakal, T. Csösz, E. Topuzov, R. Orlova, S. Tjulandin, F. Rivera, J. Straub, R. Bruns, S. Quaratino, J. Tabernero, Abituzumab combined with cetuximab plus irinotecan versus cetuximab plus irinotecan alone for patients with KRAS wild-type metastatic colorectal cancer: The randomised phase I/II POSEIDON trial. *Ann. Oncol.* **26**, 132–140 (2015).
185. M. Hussain, S. Le Moulec, C. Gimmi, R. Bruns, J. Straub, K. Miller; PERSEUS Study Group, Differential effect on bone lesions of targeting integrins: Randomised phase II trial of abituzumab in patients with metastatic castration-resistant prostate cancer. *Clin. Cancer Res.* **22**, 3192–3200 (2016).
186. H. Elbahesh, T. Cline, T. Baranovich, E. A. Govorkova, S. Schultz-Cherry, C. J. Russell, Novel roles of focal adhesion kinase in cytoplasmic entry and replication of influenza A viruses. *J. Virol.* **88**, 6714–6728 (2014).

187. M. J. A. de Jonge, N. Steeghs, M. P. Lolkema, S. J. Hotte, H. W. Hirte, D. A. J. van der Biessen, A. R. Abdul Razak, F. Y. F. L. De Vos, R. B. Verheijen, D. Schnell, L. C. Pronk, M. Jansen, L. L. Siu, Phase I study of BI 853520, an inhibitor of focal adhesion kinase, in patients with advanced or metastatic nonhematologic malignancies. *Target. Oncol.* **14**, 43–55 (2019).
188. R. Roskoski Jr., Properties of FDA-approved small molecule protein kinase inhibitors: A 2020 update. *Pharmacol. Res.* **152**, 104609 (2020).
189. L. Riva, S. Yuan, X. Yin, L. Martin-Sancho, N. Matsunaga, L. Pache, S. Burgstaller-Muehlbacher, P. D. De Jesus, P. Teriete, M. V. Hull, M. W. Chang, J. F.-W. Chan, J. Cao, V. K.-M. Poon, K. M. Herbert, K. Cheng, T.-T. H. Nguyen, A. Rubanov, Y. Pu, C. Nguyen, A. Choi, R. Rathnasinghe, M. Schotsaert, L. Miorin, M. Dejosez, T. P. Zwaka, K.-Y. Sit, L. Martinez-Sobrido, W.-C. Liu, K. M. White, M. E. Chapman, E. K. Lendy, R. J. Glynn, R. Albrecht, E. Rupp, A. D. Mesecar, J. R. Johnson, C. Benner, R. Sun, P. G. Schultz, A. I. Su, A. Garcia-Sastre, A. K. Chatterjee, K.-Y. Yuen, S. K. Chanda, Discovery of SARS-CoV-2 antiviral drugs through large-scale compound repurposing. *Nature* **586**, 113–119 (2020).
190. T. Wilkinson, R. Dixon, C. Page, M. Carroll, G. Griffiths, L.-P. Ho, A. De Soya, T. Felton, K. E. Lewis, K. Pheko, J. D. Chalmers, A. Gordon, L. McGarvey, J. Doherty, R. C. Read, M. Shankar-Hari, N. Martinez-Alier, M. O'Kelly, G. Duncan, R. Wallis, J. Sykes, C. Summers, D. Singh; ACCORD Collaborators, ACCORD: A multicentre, seamless, stage 2 adaptive randomisation platform study to assess the efficacy and safety of multiple candidate agents for the treatment of COVID-19 in hospitalised patients: A structured summary of a study protocol for a randomised controlled trial. *Trials* **21**, 691 (2020).
191. G. Lemke, Biology of the TAM receptors. *Cold Spring Harb. Perspect. Biol.* **5**, a009076 (2013).
192. M. Shimajima, Y. Ikeda, Y. Kawaoka, The mechanism of Axl-mediated Ebola virus infection. *J. Infect. Dis.* **196** (suppl. 2), S259–S263 (2007).
193. S. Mori, Y. Itoh, R. Shinohara, T. Sendo, R. Oishi, M. Nishibori, Nafamostat mesilate is an extremely potent inhibitor of human trypsinase. *J. Pharmacol. Sci.* **92**, 420–423 (2003).
194. S. A. Shiryayev, A. G. Remacle, B. I. Ratnikov, N. A. Nelson, A. Y. Savinov, G. Wei, M. Bottini, M. F. Rega, A. Parent, R. Desjardins, M. Fugere, R. Day, M. Sabet, M. Pellicchia, R. C. Liddington, J. W. Smith, T. Mustelin, D. G. Guiney, M. Lebl, A. Y. Strongin, Targeting host cell furin proprotein convertases as a therapeutic strategy against bacterial toxins and viral pathogens. *J. Biol. Chem.* **282**, 20847–20853 (2007).
195. J. A. Daniel, N. Chau, M. K. Abdel-Hamid, L. Hu, L. von Kleist, A. Whiting, S. Krishnan, P. Maamary, S. R. Joseph, F. Simpson, V. Haucke, A. McCluskey, P. J. Robinson, Phenothiazine-derived antipsychotic drugs inhibit dynamin and clathrin-mediated endocytosis. *Traffic* **16**, 635–654 (2015).
196. M. Plaze, D. Attali, A.-C. Petit, M. Blatzer, E. Simon-Loriere, F. Vinckier, A. Cachia, F. Chrétien, R. Gaillard, Repurposing chlorpromazine to treat COVID-19: The reCoVey study. *L'Encephale* **46**, 169–172 (2020).
197. K. Stadler, H. R. Ha, V. Ciminale, C. Spirli, G. Saletti, M. Schiavon, D. Bruttomesso, L. Bigler, F. Follath, A. Pettenazzo, A. Baritussio, Amiodarone alters late endosomes and inhibits SARS coronavirus infection at a post-endosomal level. *Am. J. Respir. Cell Mol. Biol.* **39**, 142–149 (2008).
198. N. Yang, H.-M. Shen, Targeting the endocytic pathway and autophagy process as a novel therapeutic strategy in COVID-19. *Int. J. Biol. Sci.* **16**, 1724–1731 (2020).
199. M. Bouhaddou, D. Memon, B. Meyer, K. M. White, V. V. Rezelj, M. C. Marrero, B. J. Polacco, J. E. Melnyk, S. Ulferts, R. M. Kaake, J. Batra, A. L. Richards, E. Stevenson, D. E. Gordon, A. Rojic, K. Obernier, J. M. Fabius, M. Soucheray, L. Miorin, E. Moreno, C. Koh, Q. D. Tran, A. Hardy, R. Robinot, T. Vallet, B. E. Nilsson-Payant, C. Hernandez-Armenta, A. Dunham, S. Weigang, J. Kner, M. Modak, D. Quintero, Y. Zhou, A. Dugourd, A. Valdeolivas, T. Patil, Q. Li, R. Hüttenhain, M. Cakir, M. Muralidharan, M. Kim, G. Jang, B. Tutuncuoglu, J. Hiatt, J. Z. Guo, J. Xu, S. Bouhaddou, C. J. P. Mathy, A. Gaulton, E. J. Manners, E. Félix, Y. Shi, M. Goff, J. K. Lim, T. McBride, M. C. O'Neal, Y. Cai, J. C. J. Chang, D. J. Broadhurst, S. Klippsten, E. De Wit, A. R. Leach, T. Kortemme, B. Shoichet, M. Ott, J. Saez-Rodriguez, B. R. tenOever, R. D. Mullins, E. R. Fischer, G. Kochs, R. Grosse, A. Garcia-Sastre, M. Vignuzzi, J. R. Johnson, K. M. Shokat, D. L. Swaney, P. Beltrao, N. J. Krogan, The global phosphorylation landscape of SARS-CoV-2 infection. *Cell* **182**, 685–712.e19 (2020).
200. M. I. Davis, A. T. Sasaki, M. Shen, B. M. Emerling, N. Thorne, S. Michael, R. Pragani, M. Boxer, K. Sumita, K. Takeuchi, D. S. Auld, Z. Li, L. C. Cantley, A. Simeonov, A homogeneous, high-throughput assay for phosphatidylinositol 5-phosphate 4-kinase with a novel, rapid substrate preparation. *PLOS ONE* **8**, e54127 (2013).
201. J.-O. De Craene, D. L. Bertazzi, S. Bär, S. Friant, Phosphoinositides, major actors in membrane trafficking and lipid signaling pathways. *Int. J. Mol. Sci.* **18**, 634 (2017).
202. E. J. Ungewickell, L. Hinrichsen, Endocytosis: Clathrin-mediated membrane budding. *Curr. Opin. Cell Biol.* **19**, 417–425 (2007).
203. P. Richardson, I. Griffin, C. Tucker, D. Smith, O. Oechsle, A. Phelan, J. Stebbing, Baricitinib as potential treatment for 2019-nCoV acute respiratory disease. *Lancet* **395**, e30–e31 (2020).
204. J. Guo, J. Zhang, L. Liang, N. Liu, M. Qi, S. Zhao, J. Su, J. Liu, C. Peng, X. Chen, H. Liu, Potent USP10/13 antagonist spautin-1 suppresses melanoma growth via ROS-mediated DNA damage and exhibits synergy with cisplatin. *J. Cell. Mol. Med.* **24**, 4324–4340 (2020).
205. R. Mateo, C. M. Nagamine, J. Spagnolo, E. Méndez, M. Rahe, M. Gale, J. Yuan, K. Kirkegaard, Inhibition of cellular autophagy deranges dengue virion maturation. *J. Virol.* **87**, 1312–1321 (2013).
206. S. Schloer, L. Brunotte, J. Goretzko, A. Mecate-Zambrano, N. Korthals, V. Gerke, S. Ludwig, U. Rescher, Targeting the endolysosomal host-SARS-CoV-2 interface by clinically licensed functional inhibitors of acid sphingomyelinase (FIASMA) including the antidepressant fluoxetine. *Emerg. Microbes Infect.* **9**, 2245–2255 (2020).
207. C.-Y. Wu, J.-T. Jan, S.-H. Ma, C.-J. Kuo, H.-F. Juan, Y.-S. E. Cheng, H.-H. Hsu, H.-C. Huang, D. Wu, A. Brik, F.-S. Liang, R.-S. Liu, J.-M. Fang, S.-T. Chen, P.-H. Liang, C.-H. Wong, Small molecules targeting severe acute respiratory syndrome human coronavirus. *Proc. Natl. Acad. Sci. U.S.A.* **101**, 10012–10017 (2004).
208. J. Kindrachuk, B. Ork, B. J. Hart, S. Mazur, M. R. Holbrook, M. B. Frieman, D. Traynor, R. F. Johnson, J. Dyall, J. H. Kuhn, G. G. Olinger, L. E. Hensley, P. B. Jahrling, Antiviral potential of ERK/MAPK and PI3K/AKT/mTOR signaling modulation for Middle East respiratory syndrome coronavirus infection as identified by temporal kinome analysis. *Antimicrob. Agents Chemother.* **59**, 1088–1099 (2015).
209. D. E. Gordon, G. M. Jang, M. Bouhaddou, J. Xu, K. Obernier, K. M. White, M. J. O'Meara, V. V. Rezelj, J. Z. Guo, D. L. Swaney, T. A. Tummino, R. Huettnerlein, R. M. Kaake, A. L. Richards, B. Tutuncuoglu, H. Foussard, J. Batra, K. Haas, M. Modak, M. Kim, P. Haas, B. J. Polacco, H. Braberg, J. M. Fabius, M. Eckhardt, M. Soucheray, M. J. Bennett, M. Cakir, M. J. McGregor, Q. Li, B. Meyer, F. Roesch, T. Vallet, A. M. Kain, L. Miorin, E. Moreno, Z. Z. C. Naing, Y. Zhou, S. Peng, Y. Shi, Z. Zhang, W. Shen, I. T. Kirby, J. E. Melnyk, J. S. Chorbha, K. Lou, S. A. Dai, I. Barrio-Hernandez, D. Memon, C. Hernandez-Armenta, J. Lyu, C. J. P. Mathy, T. Perica, K. B. Pilla, S. J. Ganesan, D. J. Saltzberg, R. Rakesh, X. Liu, S. B. Rosenthal, L. Calviello, S. Venkataraman, J. Liboy-Lugo, Y. Lin, X.-P. Huang, Y. Liu, S. A. Wankowicz, M. Bohn, M. Safari, F. S. Ugur, C. Koh, N. S. Savar, Q. D. Tran, D. Shengjuler, S. J. Fletcher, M. C. O'Neal, Y. Cai, J. C. J. Chang, D. J. Broadhurst, S. Klippsten, P. P. Sharp, N. A. Wenzell, D. Kuzuoglu, H.-Y. Wang, R. Trenker, J. M. Young, D. A. Caverio, J. Hiatt, T. L. Roth, U. Rathore, A. Subramanian, J. Noack, M. Hubert, R. M. Stroud, A. D. Frankel, O. S. Rosenberg, K. A. Verba, D. A. Agard, M. Ott, M. Emerman, N. Jura, M. von Zastrow, E. Verdin, A. Ashworth, O. Schwartz, C. d'Enfert, S. Mukherjee, M. Jacobson, H. S. Malik, D. G. Fujimori, T. Ideker, C. S. Craik, S. N. Floor, J. S. Fraser, J. D. Gross, A. Sali, B. L. Roth, D. Ruggero, J. Taunton, T. Kortemme, P. Beltrao, M. Vignuzzi, A. Garcia-Sastre, K. M. Shokat, B. K. Shoichet, N. J. Krogan, A SARS-CoV-2 protein interaction map reveals targets for drug repurposing. *Nature* **583**, 459–468 (2020).
210. Y.-M. Wei, X. Li, M. Xu, J. M. Abais, Y. Chen, C. R. Riebling, K. M. Boini, P.-L. Li, Y. Zhang, Enhancement of autophagy by simvastatin through inhibition of Rac1-mTOR signaling pathway in coronary arterial myocytes. *Cell. Physiol. Biochem.* **31**, 925–937 (2013).
211. W. Gu, R. Cui, T. Ding, X. Li, J. Peng, W. Xu, F. Han, X. Guo, Simvastatin alleviates airway inflammation and remodelling through up-regulation of autophagy in mouse models of asthma. *Respirology* **22**, 533–541 (2017).
212. H. Cai, R. R. Reed, Cloning and characterization of neuropilin-1-interacting protein: A PSD-95/Dlg/ZO-1 domain-containing protein that interacts with the cytoplasmic domain of neuropilin-1. *J. Neurosci.* **19**, 6519–6527 (1999).
213. H. El Mourabit, P. Poinat, J. Koster, H. Sondermann, V. Wixler, E. Wegener, E. Laplantine, D. Geerts, E. Georges-Labouesse, A. Sonnenberg, M. Aumailley, The PDZ domain of TIP-2/GIPC interacts with the C-terminus of the integrin $\alpha 5$ and $\alpha 6$ subunits. *Matrix Biol.* **21**, 207–214 (2002).
214. C. Gao, J. Zeng, N. Jia, K. Stavenhagen, Y. Matsumoto, H. Zhang, J. Li, A. J. Hume, E. Mühlberger, I. van Die, J. Kwan, K. Tantisira, A. Emili, R. D. Cummings, SARS-CoV-2 spike protein interacts with multiple innate immune receptors. *bioRxiv* 2020.07.29.227462 [Preprint]. 30 July 2020. <https://doi.org/10.1101/2020.07.29.227462>.
215. M. Roschewski, M. S. Lionakis, J. P. Sharman, J. Roswarski, A. Goy, M. A. Monticelli, M. Roshon, S. H. Wrzesinski, J. V. Desai, M. A. Zarakas, J. Collen, K. Rose, A. Hamdy, R. Izumi, G. W. Wright, K. K. Chung, J. Basella, L. M. Staudt, W. H. Wilson, Inhibition of Bruton tyrosine kinase in patients with severe COVID-19. *Sci. Immunol.* **5**, eabd0110 (2020).
216. M. Bassetti, N. Castaldo, A. Carnelutti, Neuraminidase inhibitors as a strategy for influenza treatment: Pros, cons and future perspectives. *Expert Opin. Pharmacother.* **20**, 1711–1718 (2019).
217. M. Solmi, A. Murru, I. Pacchiarotti, J. Undurraga, N. Veronese, M. Fornaro, B. Stubbs, F. Monaco, E. Vieta, M. V. Seeman, C. U. Correll, A. F. Carvalho, Safety, tolerability, and risks associated with first- and second-generation antipsychotics: A state-of-the-art clinical review. *Ther. Clin. Risk Manag.* **13**, 757–777 (2017).
218. F. Zhou, T. Yu, R. Du, G. Fan, Y. Liu, Z. Liu, J. Xiang, Y. Wang, B. Song, X. Gu, L. Guan, Y. Wei, H. Li, X. Wu, J. Xu, S. Tu, Y. Zhang, H. Chen, B. Cao, Clinical course and risk factors for mortality of adult inpatients with COVID-19 in Wuhan, China: A retrospective cohort study. *Lancet* **395**, 1054–1062 (2020).
219. G. S. Horan, S. Wood, V. Ona, D. J. Li, M. E. Lukashev, P. H. Weinreb, K. J. Simon, K. Hamm, N. E. Allaire, N. J. Rinaldi, J. Goyal, C. A. Feghali-Bostwick, E. L. Matteson, C. O'Hara, R. Lafyatis, G. S. Davis, X. Huang, D. Sheppard, S. M. Violette, Partial inhibition of integrin $\alpha v \beta 6$ prevents pulmonary fibrosis without exacerbating inflammation. *Am. J. Respir. Crit. Care Med.* **177**, 56–65 (2008).

220. A. E. John, R. H. Graves, K. T. Pun, G. Vitulli, E. J. Forty, P. F. Mercer, J. L. Morrell, J. W. Barrett, R. F. Rogers, M. Hafeji, L. I. Bibby, E. Gower, V. S. Morrison, Y. Man, J. A. Roper, J. C. Luckett, L. A. Borthwick, B. S. Barksby, R. A. Burgoyne, R. Barnes, J. Le, D. J. Flint, S. Pyne, A. Habgood, L. A. Organ, C. Joseph, R. C. Edwards-Pritchard, T. M. Maher, A. J. Fisher, N. S. Gudmann, D. J. Leeming, R. C. Chambers, P. T. Lukey, R. P. Marshall, S. J. F. Macdonald, R. G. Jenkins, R. J. Slack, Translational pharmacology of an inhaled small molecule α v β 6 integrin inhibitor for idiopathic pulmonary fibrosis. *Nat. Commun.* **11**, 4659 (2020).
221. D. Bojkova, K. Klann, B. Koch, M. Widera, D. Krause, S. Ciesek, J. Cinatl, C. Münch, Proteomics of SARS-CoV-2-infected host cells reveals therapy targets. *Nature* **583**, 469–472 (2020).
222. A. Stukalov, V. Girault, V. Grass, V. Bergant, O. Karayel, C. Urban, D. A. Haas, Y. Huang, L. Oubraham, A. Wang, S. M. Hamad, A. Piras, M. Tanzer, F. M. Hansen, T. Engheleitner, M. Reinecke, T. M. Lavacca, R. Ehmann, R. Wölfel, J. Jores, B. Kuster, U. Protzer, R. Rad, J. Ziebuhr, V. Thiel, P. Scaturro, M. Mann, A. Pichlmair, Multi-level proteomics reveals host-perturbation strategies of SARS-CoV-2 and SARS-CoV. *bioRxiv* 2020.06.17.156455 [Preprint]. 17 June 2020. <https://doi.org/10.1101/2020.06.17.156455>.
223. UniProt Consortium, UniProt: A worldwide hub of protein knowledge. *Nucleic Acids Res.* **47**, D506–D515 (2019).
224. D. A. Benson, M. Cavanaugh, K. Clark, I. Karsch-Mizrachi, D. J. Lipman, J. Ostell, E. W. Sayers, GenBank. *Nucleic Acids Res.* **41**, D36–D42 (2013).
225. F. Sievers, D. G. Higgins, Clustal Omega, accurate alignment of very large numbers of sequences. *Methods Mol. Biol.* **1079**, 105–116 (2014).
226. A. M. Waterhouse, J. B. Procter, D. M. A. Martin, M. Clamp, G. J. Barton, Jalview Version 2—A multiple sequence alignment editor and analysis workbench. *Bioinformatics* **25**, 1189–1191 (2009).
227. H. M. Berman, J. Westbrook, Z. Feng, G. Gilliland, T. N. Bhat, H. Weissig, I. N. Shindyalov, P. E. Bourne, The protein data bank. *Nucleic Acids Res.* **28**, 235–242 (2000).
228. C. C. Huang, E. C. Meng, J. H. Morris, E. F. Pettersen, T. E. Ferrin, Enhancing UCSF Chimera through web services. *Nucleic Acids Res.* **42**, W478–W484 (2014).
229. T. Teesalu, K. N. Sugahara, V. R. Kotamraju, E. Ruoslahti, C-end rule peptides mediate neuropilin-1-dependent cell, vascular, and tissue penetration. *Proc. Natl. Acad. Sci. U.S.A.* **106**, 16157–16162 (2009).
230. A. Fantin, Q. Schwarz, K. Davidson, E. M. Normando, L. Denti, C. Ruhrberg, The cytoplasmic domain of neuropilin 1 is dispensable for angiogenesis, but promotes the spatial separation of retinal arteries and veins. *Development* **138**, 4185–4191 (2011).
231. U. Yaqoob, S. Cao, U. Shergill, K. Jagavelu, Z. Geng, M. Yin, T. M. de Assuncao, Y. Cao, A. Szabolcs, S. Thorgeirsson, M. Schwartz, J. D. Yang, R. Ehman, L. Roberts, D. Mukhopadhyay, V. H. Shah, Neuropilin-1 stimulates tumor growth by increasing fibronectin fibril assembly in the tumor microenvironment. *Cancer Res.* **72**, 4047–4059 (2012).
232. H. L. Goel, A. M. Mercurio, Enhancing integrin function by VEGF/neuropilin signaling: Implications for tumor biology. *Cell Adh. Migr.* **6**, 554–560 (2012).
233. H. L. Goel, B. Pursell, C. Standley, K. Fogarty, A. M. Mercurio, Neuropilin-2 regulates α 6 β 1 integrin in the formation of focal adhesions and signaling. *J. Cell Sci.* **125**, 497–506 (2012).
234. T. S. Ellison, S. J. Atkinson, V. Steri, B. M. Kirkup, M. E. J. Preedy, R. T. Johnson, C. Ruhrberg, D. R. Edwards, J. G. Schneider, K. Weilbaecher, S. D. Robinson, Suppression of β 3-integrin in mice triggers a neuropilin-1-dependent change in focal adhesion remodelling that can be targeted to block pathological angiogenesis. *Dis. Model. Mech.* **8**, 1105–1119 (2015).
235. Y.-J. Kim, K. Jung, D.-S. Baek, S.-S. Hong, Y.-S. Kim, Co-targeting of EGF receptor and neuropilin-1 overcomes cetuximab resistance in pancreatic ductal adenocarcinoma with integrin β 1-driven Src-Akt bypass signaling. *Oncogene* **36**, 2543–2552 (2017).

Acknowledgments: We thank J. Kliche, H. Kuss, M. Ali, and Y. Ivarsson from the Uppsala University for testing several motif candidates and sharing their peptide-domain binding data in advance of publication. We thank S. Michael for helping to prepare the ELM entry LIG_NRP_CendR_1. We are grateful to G. Jenkins and the Nottingham Covid Research Group for making integrin and ACE2 data publicly available on laboratory website (<https://www.nottinghamcrng.info/results>). **Funding:** B.M. has received funding from the European Union's Horizon 2020 research and innovation programme under the Marie Skłodowska-Curie grant agreement no. 842490 (MIMIC). J.Č. is supported by the European Union's Horizon 2020 research and innovation programme under the Marie Skłodowska-Curie grant agreement no. 675341 (PDZnet). E.M.-P. is a PhD student of CONICET, Argentina. R.A. is supported by BMBF-funded Heidelberg Center for Human Bioinformatics (HD-HuB) within the German Network for Bioinformatics Infrastructure (de.NBI #031A537B) and ELIXIR Germany. L.B.C. is a National Research Council Investigator (CONICET, Argentina). The work was supported by Agencia Nacional de Promoción Científica y Tecnológica (PICT 2017-1924) grant to L.B.C. This paper is part of a project that has received funding from the European Union's Horizon 2020 research and innovation programme under the Marie Skłodowska-Curie grant agreement no. 778247 (IDPfun) to L.B.C., D.C.S., and T.J.G. IDPfun also funded E.M.-P.'s placement at EMBL.

Author contributions: All authors worked on the manuscript as it evolved and contributed to the regular discussions by teleconference. B.M. (ORCID: 0000-0003-0919-4449) identified and analyzed integrin-related SLiMs, analyzed sequence and structural data, prepared the corresponding alignments and structural figures, and wrote the sections related to integrins. H.S.-S. (ORCID: 0000-0003-4744-4787) contributed to the introduction, the NPY and SH2 motif sections, and the discussion on tyrosine kinase inhibitors. J.A.-V. (ORCID: 0000-0003-0752-1151) prepared sequence alignments and figures. J.Č. (ORCID: 0000-0003-1047-4157) analyzed the ACE2 PBM and wrote the related results section. E.M.-P. (ORCID: 0000-0003-4411-976X) prepared the figure of phosphorylation of ACE2 tail (literature searches for phosphorylation of ACE2 tail). R.A. (ORCID: 0000-0002-7212-0234) undertook literature searches, maintained the reference database, and coordinated with B.M. to meet submission requirements. D.C.S. (ORCID: 0000-0003-4015-2474) worked on the RGD and integrin aspects. M.K. (ORCID: 0000-0002-3004-2151) worked on defining regular expression for autophagy (LIR autophagy), wrote LIR autophagy motif section, contributed toward developing drugs table, and wrote parts of the introduction, therapeutics, and discussion section. F.R. (ORCID: 0000-0002-4604-9251) provided cilengitide aspects, including development history, and assessments of other drugs, in the therapeutics section, and discussion. L.B.C. (ORCID: 0000-0003-0192-9906) worked on the identification and definition of ACE2 tail motifs, the assessment of the switching mechanisms acting on the ACE2 tail, and the assessment of drugs targeting viral entry; participated in figure design; and wrote several sections of the introduction, results, and the discussion. T.J.G. (ORCID: 0000-0003-0657-5166) undertook SLiM searches and evaluations, prepared sequence alignments, and wrote the YxxPhi section and parts of the results, introduction, and discussion. **Competing interests:** F.R. has worked on integrin inhibitors in Merck KGaA, Darmstadt, Germany. All other authors declare that they have no competing interests. **Data and materials availability:** All data needed to evaluate the conclusions in the paper are present in the paper or the Supplementary Materials.

Submitted 28 May 2020

Accepted 10 December 2020

Published 12 January 2021

10.1126/scisignal.abd0334

Citation: B. Mészáros, H. Sámano-Sánchez, J. Alvarado-Valverde, J. Čalyševa, E. Martínez-Pérez, R. Alves, D. C. Shields, M. Kumar, F. Rippmann, L. B. Chemes, T. J. Gibson, Short linear motif candidates in the cell entry system used by SARS-CoV-2 and their potential therapeutic implications. *Sci. Signal.* **14**, eabd0334 (2021).